A new interactive chemistry-climate model: 2. Sensitivity of the middle atmosphere to ozone depletion and increase in greenhouse gases and implications for recent stratospheric cooling

E. Manzini,[1,2] B. Steil,[3] C. Brühl,[3] M. A. Giorgetta,[1] and K. Krüger[4]

Received 24 September 2002; revised 30 January 2003; accepted 24 March 2003; published 29 July 2003.

[1] The sensitivity of the middle atmosphere circulation to ozone depletion and increase in greenhouse gases is assessed by performing multiyear simulations with a chemistry-climate model. Three simulations with fixed boundary conditions have been carried out: one simulation for the near-past (1960) and two simulations for the near-present (1990 and 2000) conditions, including changes in greenhouse gases, in total organic chlorine, and in average sea surface temperatures. Changes in ozone are simulated interactively by the coupled model. It is found that in the stratosphere, ozone decreases, and that in the Antarctic, the ozone hole develops in both the 1990 and the 2000 simulations but not in the 1960 simulation, as observed. The simulated temperature decreases in the stratosphere and mesosphere from the near past to the present, with the largest changes at the stratopause and at the South Pole in the lower stratosphere, in agreement with current knowledge of temperature trends. In the Arctic lower stratosphere, a cooling in March with respect to the 1960 simulation is found only for the 2000 simulation. Wave activity emerging from the troposphere is found to be comparable in the winters of the 1960 and 2000 simulations, suggesting that ozone depletion and greenhouse gases increase contribute to the 2000–1960 March cooling in the Arctic lower stratosphere. These results therefore provide support to the interpretation that the extreme low temperatures observed in March in the last decade can arise from radiative and chemical processes, although other factors cannot be ruled out. The comparison of the 1960 and 2000 simulations shows an increase in downwelling in the mesosphere at the time of cooling in the lower stratosphere (in March in the Arctic; in October in the Antarctic). The mesospheric increase in downwelling can be explained as the response of the gravity waves to the stronger winds associated with the cooling in the lower stratosphere. Planetary waves appear to contribute to the downward shift of the increased downwelling, with a delay of about a month. The increase in dynamical heating associated with the increased downwelling may limit the cooling and the strengthening of the lower stratospheric polar vortex from above, facilitating ozone recovery and providing a negative dynamical feedback. In both the Arctic and Antarctic the cooling from ozone depletion is found to affect the area covered with polar stratospheric clouds in spring, which is substantially increased from the 1960 to the 2000 simulations. In turn, increased amounts of polar stratospheric clouds can facilitate further ozone depletion in the 2000 simulation. *INDEX TERMS:* 0340 Atmospheric Composition and Structure: Middle atmosphere—composition and chemistry; 0341 Atmospheric Composition and Structure: Middle atmosphere—constituent transport and chemistry (3334); 3334 Meteorology and Atmospheric Dynamics: Middle atmosphere dynamics (0341, 0342); *KEYWORDS:* chemistry-climate model, middle atmosphere dynamics, gravity waves, ozone depletion, global change, polar ozone

Citation: Manzini, E., B. Steil, C. Brühl, M. A. Giorgetta, and K. Krüger, A new interactive chemistry-climate model: 2. Sensitivity of the middle atmosphere to ozone depletion and increase in greenhouse gases and implications for recent stratospheric cooling, *J. Geophys. Res.*, *108*(D14), 4429, doi:10.1029/2002JD002977, 2003.

[1]Max-Planck-Institut für Meteorologie, Hamburg, Germany.
[2]Now at National Institute for Geophysics and Volcanology, Bologna, Italy.
[3]Max-Planck-Institut für Chemie, Mainz, Germany.
[4]Freie Universität Berlin, Berlin, Germany.

0148-0227/03/2002JD002977

1. Introduction

[2] Recently, the *Ramaswamy et al.* [2001] review on the status of stratospheric trends has provided evidence that globally the stratosphere has been cooling in the last decades, although the rate of cooling appears to depend on the length of record and the part of the globe considered.

The southern polar latitudes have experienced a cooling trend since the 1980s, while the northern polar latitudes show instead the most pronounced changes in the last decade (e.g., the 1990s).

[3] Concerning the polar stratosphere, it is nowadays accepted that chemically driven ozone depletion is a dominant cause behind the reported temperature trends in the Southern Hemisphere, as reviewed by *Solomon* [1999]. It is also established that the radiative response to polar ozone depletion is a cooling of the lower stratosphere that in turn may enhance the ozone depletion, because heterogeneous chemistry responsible for the depletion is more effective at lower temperatures. This mechanism can provide a positive radiative-chemical feedback [*Shine*, 1986; *Randel and Wu*, 1999a].

[4] Given the large variability of the Northern Hemisphere circulation, it is possible that changes in atmospheric composition, variations in internal dynamics, and external forcing all play a role in the cooling of the lower stratosphere. However, their respective contribution is uncertain at present. In particular, it is subject of current research to determine the response and the sensitivity of the stratospheric circulation to atmospheric composition changes. For instance, it is currently debated whether dynamical processes can enhance or dampen changes in temperatures due to changes in atmospheric compositions. The works of *Austin et al.* [1992] and *Shindell et al.* [1998] have suggested that the dynamical response to increase in greenhouse gases and ozone depletion occurring together can exacerbate the conditions for ozone depletion in the Northern Hemisphere. According to these works, the radiative cooling of the lower stratosphere due to the increase in greenhouse gases and ozone depletion may result in a more stable polar vortex. In turn, a more stable vortex can alter planetary wave propagation so that less stratospheric warming events will occur, resulting in further cooling of the polar stratosphere. However, although it is clear that an increase in greenhouse gases has a direct impact on the stratosphere by means of radiative cooling, some recent modeling studies [*Butchart and Scaife*, 2001; *Schnadt et al.*, 2001; *Gillett et al.*, 2002] suggest that it can also lead to increased planetary wave activity emanating from the troposphere, possibly favoring stratosphere planetary wave breaking and in turn increased polar downwelling and heating of the polar stratosphere.

[5] Since the discovery of the ozone hole in Antarctica [*Farman et al.*, 1985] a body of literature has developed on the problem of ozone depletion. Early investigations dealt with the identification of the processes leading to the ozone depletion and established the role of chlorine species and heterogeneous chemistry as the primary cause of the depletion; for an extensive review, see *Solomon* [1999]. The simulation of ozone depletion and its impacts with general circulation models (GCMs) generally involves some degree of simplifications. For instance, upper stratospheric and mesospheric processes are not included by *Schnadt et al.* [2001], and highly parameterized chemistry is used in the works of *Mahlman et al.* [1994] and *Shindell et al.* [1998]. Another approach is to specify the ozone changes, for instance the early works of *Fels et al.* [1980] and *Kiehl et al.* [1988]. For a review on recent model simulated trends, see *Shine et al.* [2003], and for a summary of the current status of modeling, see *Austin et al.* [2003]. Comprehensive simulations with a detailed stratospheric chemical model coupled to a GCM have been performed recently by *Austin* [2002] and *Austin et al.* [2000, 2001], among a few others. However, these works have been restricted to single and/or relatively short term integrations, limiting their effectiveness because of the large internal interannual variability of the atmosphere. A climatological study has been recently presented by *Rozanov et al.* [2001].

[6] The purpose of this work is to use an interactive chemistry climate model to address the sensitivity of the middle atmosphere to the main composition changes that occurred from the pre-ozone hole (near past) to the present time, specifically the increase in greenhouse gases and the ozone depletion. The chemistry climate model consists of a state-of-the-art GCM that includes the middle atmosphere fully coupled to a chemical model of stratospheric ozone that includes both homogenous and heterogeneous chemistry [*Steil et al.*, 2003]. Given that the model is interactive, it is possible to simulate the feedback among chemical, radiative and dynamical processes that determine the changes in the simulated polar lower stratospheric temperature. The aim is to use the model results to gain an understanding of the causes of the observed polar stratospheric cooling, especially in the Northern Hemisphere where the dynamical role is uncertain at present.

[7] A novel aspect of this work is to take into account the large interannual variability of the atmosphere, by performing simulations lasting many years with selected fixed boundary conditions. Namely, results are presented from three simulations, each 20 years long after spin up. The first simulation is characterized by low chlorine and greenhouse gases concentrations (as typical for near-past conditions, 1960) and is contrasted to two simulations with chlorine and greenhouse gases concentrations respectively of the beginning and the late 1990s (as typical for present conditions). In addition, average changes in sea surface temperatures are taken into account. The climatology and interannual variability of the simulations with near-present conditions have been compared to HALOE/UARS observations by *Steil et al.* [2003].

[8] First, we characterize and evaluate ozone and temperature changes related to the changes in the chemical processes acting in the near-past and present conditions, namely activation of heterogeneous chemistry due to the increase in total organic chlorine in the two present simulations with respect to the past simulation. The ozone and temperature changes are compared with estimates from observations, in order to establish a degree of confidence in the changes produced by the model. Second, changes in the residual circulation and other diagnostics (heat fluxes, EP-fluxes, sudden stratospheric warming events) of dynamical processes are addressed in order to evaluate the dynamical response simulated by the model.

[9] Section 2 briefly describes the chemistry climate model and presents the design of the simulations. Changes in annual and zonal mean distributions of basic fields are reported in section 3. Section 4 deals with average ozone changes. Section 5 is dedicated to the changes in temperature and to the feedback from dynamical processes. The focus in section 5 is on the polar regions. In section 6 the changes in chlorine partitioning, polar stratospheric clouds (PSCs) and other chemical aspects are discussed. The

Table 1. Definition of the Simulations

	1960 Simulation	1990 Simulation	2000 Simulation
CH_4 mixing ratio	1.26 ppmv	1.69 ppmv	1.75 ppmv
N_2O mixing ratio	295 ppbv	310 ppbv	320 ppbv
CO_2 mixing ratio	317 ppmv	353 ppmv	372 ppmv
Organic Cl mixing ratio	0.8 ppbv	3.4 ppbv	3.7 ppbv
GISS Hadley SST	(1951–1960) average	(1981–1990) average	(1989–1998) average

interannual variability present in the simulations is reported in section 7. In section 8, conclusions are drawn.

2. Interactive Chemistry Climate Model and Design of Simulations

[10] The chemistry climate model used is the MAECHAM4/CHEM model presented by *Steil et al.* [2003] (hereinafter referred to as part 1). MAECHAM4 is a general circulation model of the atmosphere extending from the surface to 0.01 hPa (~80 km), including state-of-the-art physical parameterizations for the radiative transfer and gravity wave processes which allow for a reasonably realistic simulation of the middle atmosphere circulation at middle and high latitudes [*Manzini et al.*, 1997; *Manzini and McFarlane*, 1998]. These processes are directly relevant for the interpretation of the changes reported below. Of specific interest is the parameterization of the momentum flux deposition due to a spectrum of gravity waves [*Hines*, 1997a, 1997b]. At the source level, in the troposphere, a continuous and isotropic spectrum of gravity waves in 8 azimuths is specified. The isotropic condition implies that the vertical flux of horizontal momentum carried by the waves in each azimuth is the same. Therefore the net flux in the cardinal directions at the source level is zero. The parameterization thereafter takes into account the propagation, breaking and dissipation of the waves in the background large-scale flow simulated by the model. Breaking and dissipation may occur by increase of wave amplitude with elevation (because of the compressibility of air), critical level interaction with the background flow, and nonlinear Doppler spreading, following *Hines* [1997a]. In the tropical stratosphere the quasi-biennial oscillation in zonal winds does not spontaneously appear in the MAECHAM4 model.

[11] The resolution of the MAECHAM4 model is T30 horizontal truncation and 39 vertical levels, spanning the troposphere, stratosphere and mesosphere. The vertical resolution is finer in the lower part of the atmosphere, being about 1.5–2 km in the lower stratosphere.

[12] CHEM is the module that simulates the photochemical processes relevant to the stratospheric ozone, including heterogeneous chemistry [*Steil et al.*, 1998]. Polar stratospheric clouds are explicitly calculated, from the simulated temperature, water vapor and HNO_3. The simulation of ozone in the polar lower stratosphere with MAECHAM4/CHEM for present conditions has been presented in part 1. The chemical compounds, affected by dynamics via transport and mixing and by temperature, feed back on the general circulation by changing the distributions of the radiative active trace gases (e.g., ozone and water vapor) in the radiative transfer calculation. Chemical species are advected using the flux-form semi-Lagrangian transport scheme SPITFIRE [*Rasch and Lawrence*, 1998; see also part 1].

[13] Results are presented for three equilibrium simulations, each one lasting 20 years after spin-up. Therefore the changes reported in the following sections are based on 20-year means of the fields considered. Each simulation is characterized by fixed lower boundary conditions for chemically active source gases and major greenhouse gases [*World Meteorological Organization* (*WMO*), 1999]. Namely, mixing ratios are defined at the surface for CH_4, N_2O, and total organic Cl. Their distributions in the atmosphere are obtained from the model by transport and chemical processes. The mixing ratio for CO_2 is instead a constant throughout the atmosphere. Monthly climatological sea surface temperatures (SSTs) are specified for each simulation. The use of different decadal averages for each simulation takes into account average SST changes due to the increase of greenhouse gases, generally a warming in the tropics of half a degree. The SST interannual variability (for instance, the variability associated with the El Nino Southern Oscillation phenomenon) is instead excluded in the boundary forcing of the simulations. The boundary conditions of the three simulations are chosen to represent typical conditions respectively for the near past (hereafter the 1960 simulation), early 1990s (hereafter the 1990 simulation) and late 1990s (hereafter the 2000 simulation) as summarized in Table 1. The CO_2 change is ~15% from 1960 to 1990, the total chlorine increase of a factor 4 from 1960 to 1990, and ~10% from 1990 to 2000. Note that the imposed total chlorine increase in mixing ratio at the surface results in a comparable increase of total chlorine also in the lower stratosphere.

3. Annual and Zonal Mean Changes

[14] The percentage change in ozone between the 1960 and 2000 simulations for the 20-year mean of the annual, zonal mean is shown in Figure 1 (top left). It is statistically significant at the 99% level almost everywhere. In the middle atmosphere the simulated ozone change is almost everywhere negative and its pattern is consistent with reported trends from various measurements [*World Climate Research Program-Stratospheric Processes and their Role in Climate* (*WCRP-SPARC*), 1998; *Randel and Wu*, 1999b; *WMO*, 1995, Figure 1.13]: Large relative depletions (more than 20%) are found in the middle and high latitudes in the upper stratosphere (a symmetric feature with respect to the equator) and in the lowermost polar stratosphere, at the South Pole. The latter peaks at 90 hPa (~35%) and is the ozone hole, due to heterogeneous chemistry activated by the increase in total organic chlorine (examples shown in section 6). Note that polar ozone depletion is a seasonal feature, as illustrated in Figures 2

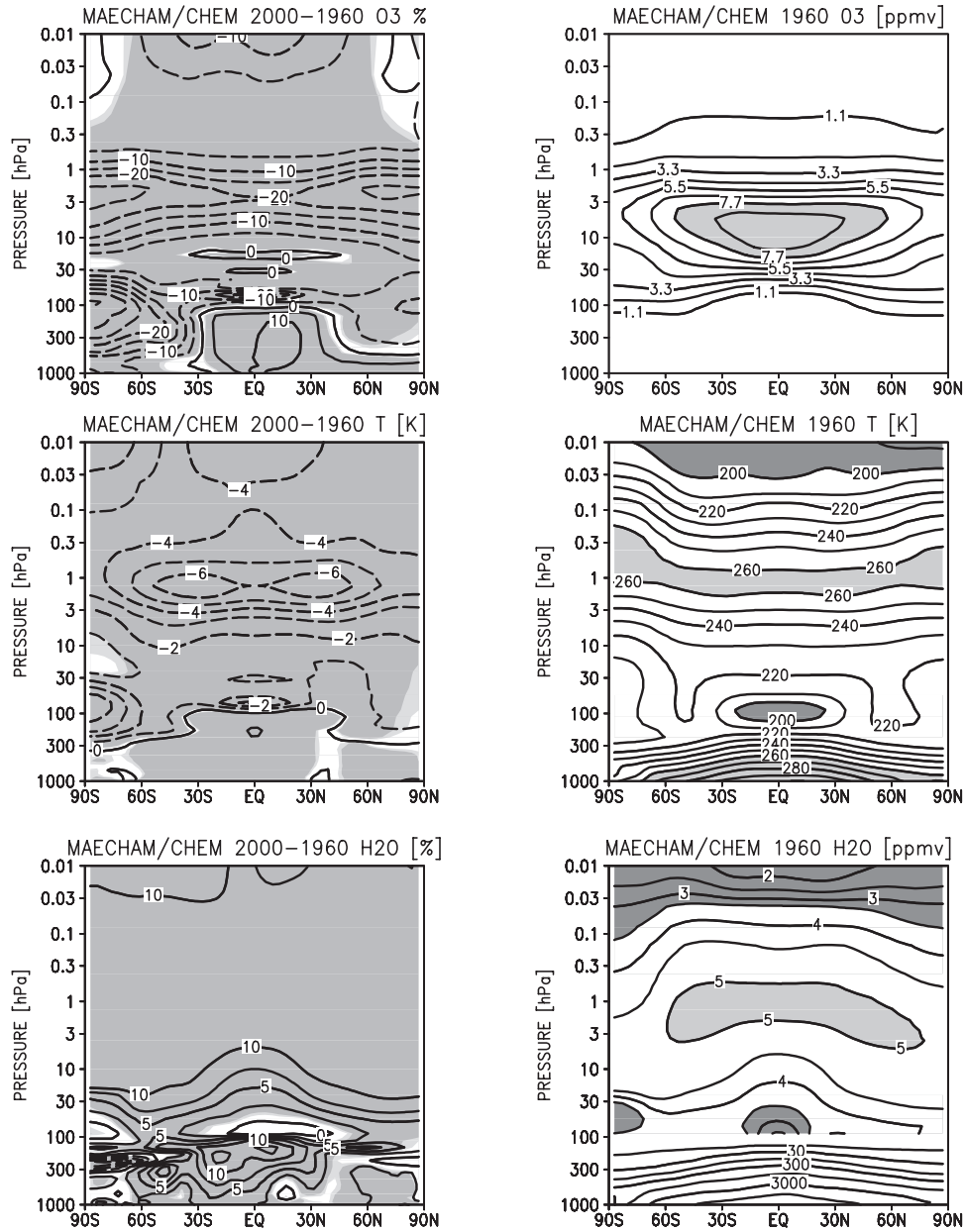

Figure 1. Annual, zonal mean ozone (top), temperature (middle), and water vapor (bottom). (right) 20-year averages from the 1960 simulation. (left) Difference, 2000–1960, between the 20-year averages of the 1960 and 2000 simulations. Left panels: dark (light) shades denote significance at 99% (95%) level. Contours: (top left) 5%; (top right) 1.1 ppmv, light shade > 7.7 ppmv; (middle left) 1 K; (middle right) 10 K, light shade > 260 K, dark shade < 200 K; (bottom left) 2.5%; (bottom right) for pressure < 100 hPa: 0.5 ppmv, light shade > 5 ppmv and dark shade < 3.5 ppmv; elsewhere: 10, 30, 100, 300, 1000, 3000, 10000 ppmv.

and 3 and in the following sections. In model and observations there is also a large ozone decrease just above the tropical tropopause. In the upper stratosphere, the ozone change pattern is a signature of depletion from homogeneous chemistry. As reviewed by *Solomon* [1999], the upper stratosphere equatorial minimum in ozone depletion is related to the role of methane (more abundant in the tropics because methane is directly advected upward from the troposphere) in maintaining chlorine in the reservoir form, HCl. The ozone changes we obtain are also consistent with the results from *Austin* [2002], who performed a single transient simulation with an interactive chemistry climate model for the last 20 years (therefore not directly comparable to our simulation design). In the upper stratosphere, where ozone is controlled by homogeneous chemistry, the results of this paper and *Austin* [2002] also compare quantitatively, while differences are found in the lower stratosphere, where heterogeneous chemistry is responsible for the depletion. Our ozone changes in the stratosphere are also consistent with the ozone change estimates from 1980–

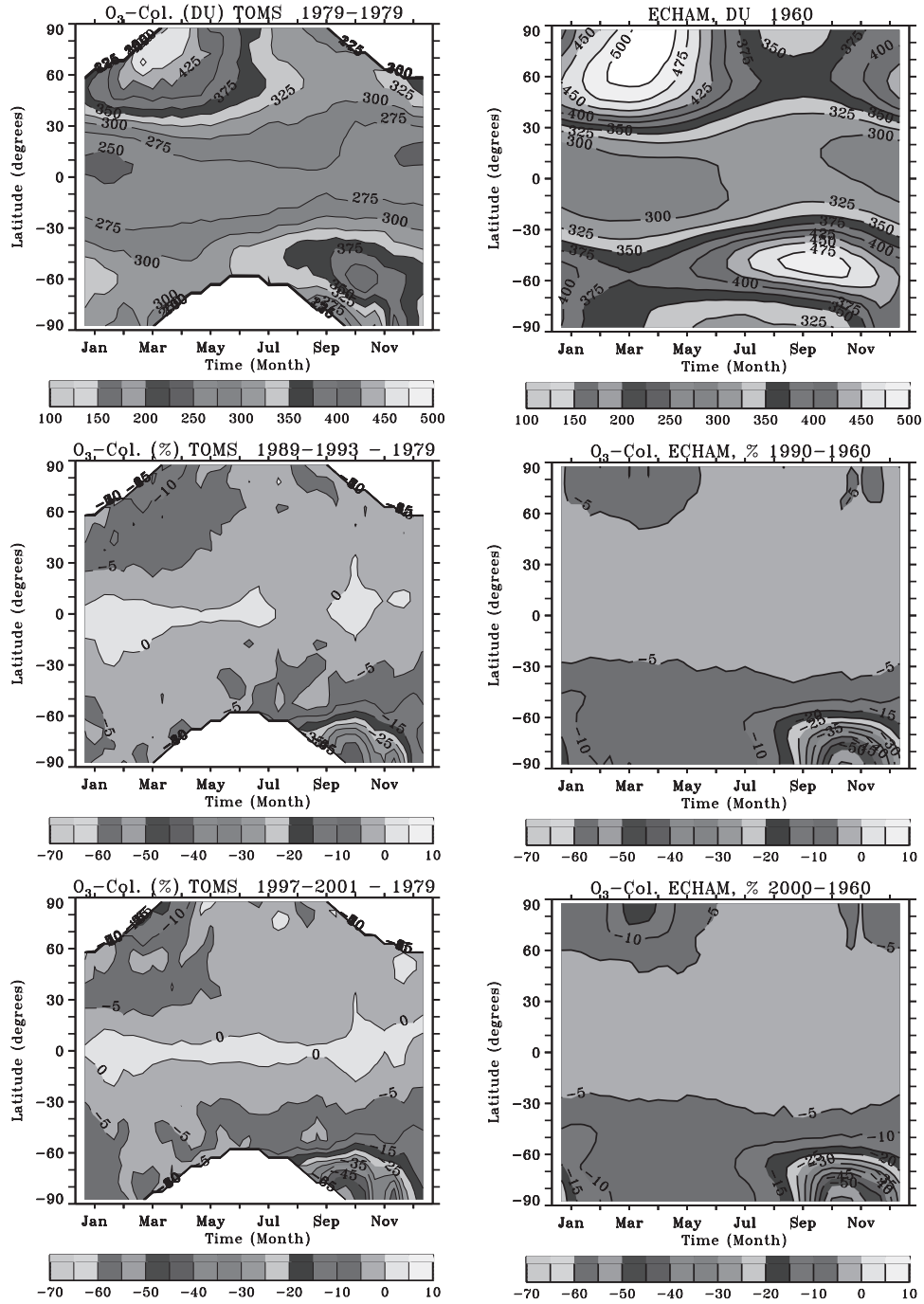

Figure 2. Ten-day mean, zonal mean of total ozone from (left) TOMS observations and (right) the simulations. (top left) 1979 year from TOMS and (top right) 20-year average from the 1960 simulation (contour: 25 DU). Difference (middle left) between the 1989 to 1993 average and the 1979 year, from TOMS and (middle right) between the 20-year averages of the 1960 and 1990 simulations, 1990–1960. Difference (bottom left) between the 1997 to 2001 average and the 1979 year, from TOMS and (bottom right) between the 20-year averages of the 1960 and 2000 simulations, 2000–1960. The difference fields are in percent, and the contour is 5%.

1996 for northern midlatitudes reported by *WMO* [1999, Figure 6.1]. Note that the conversion factor from absolute ozone differences to trends per decade is altitude dependent. At 40 km homogeneous ozone destruction by chlorine, which is linear, is important for the difference. There the factor is approximately 1/3 (three decades, neglecting the small amount of chorine during the 1960s). In the lower stratosphere the factor is approximately 1/1.5, because heterogeneous ozone destruction is nonlinear and the amount of total anorganic chlorine has to reach values higher than approximately 2.2 ppbv to be really effective, as happened in the early 1980s. For reference, the 1960

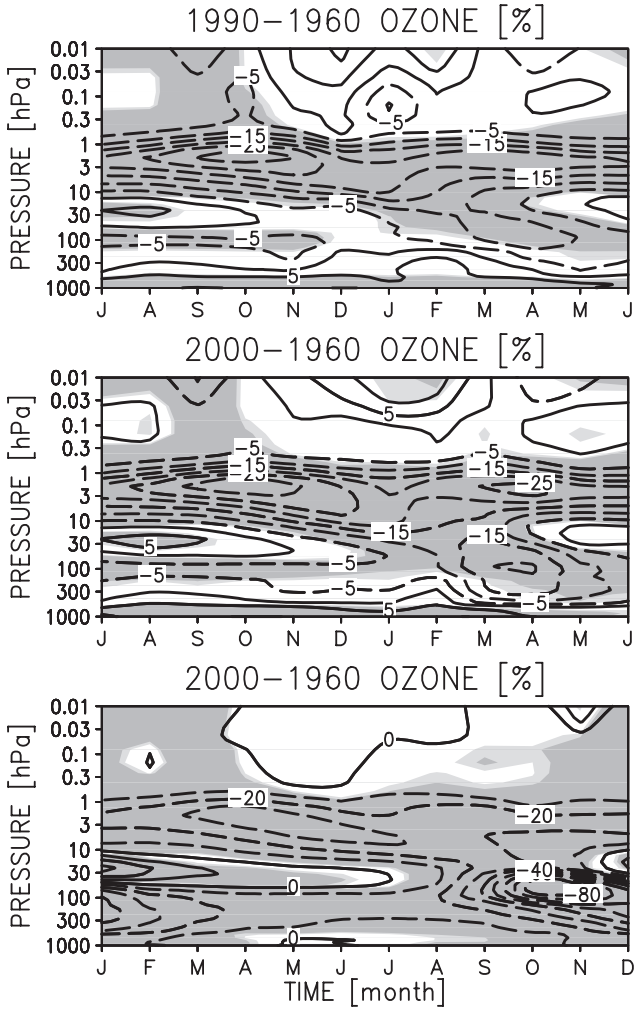

Figure 3. Difference of the monthly, zonal mean ozone (top) between the 20-year averages of the 1960 and 1990 simulations, 1990–1960, at 80°N; (middle) the 20-year averages of the 1960 and 2000 simulations, 2000–1960, at 80°N; (bottom) the 20-year averages of the 1960 and 2000 simulations, 2000–1960, at 80°S. Contour: 5% (top and middle); 10% (bottom). Dark (light) shades denote significance at 99% (95%) level.

ozone field as simulated from the model is shown in Figure 1, top right.

[15] The increase in greenhouse gases and the ozone depletion perturb the simulated average state of the atmosphere globally, as illustrated in Figure 1 (middle left) by the annual-zonal mean change in temperature, between the 2000 and the 1960 simulations. The temperature change is statistically significant at the 99% level almost everywhere. Figure 1 shows that the model troposphere warms and the middle atmosphere cools, as expected from the change in radiative forcing between the two simulations. The warming of the troposphere is relatively small, because of the small increase in greenhouse gases considered. The cooling of the middle atmosphere is largest at the stratopause. Other parts of the atmosphere where the temperature change is relatively large are the southern polar lower stratosphere and the region just above the tropical tropopause.

[16] Given that the atmosphere may not have been perturbed uniformly in time in the last 40 years, the temperature change from Figure 1 is not directly comparable to temperature trends derived from a shorter data set, like that shown by *Ramaswamy et al.* [2001, Figure 5b]. It is nevertheless of interest to compare the pattern of change. The simulated increase with elevation of the temperature change in the stratosphere is consistent with the temperature trend from satellite observation reported by *Ramaswamy et al.* [2001]. In the Southern Hemisphere, the linear trend (about −1.5 K/decade) deduced from the model at the stratopause also agrees in magnitude with that reported in the review by *Ramaswamy et al.* [2001]. However, in our model the change at the stratopause is quite symmetric with respect to the equator, while in the work of *Ramaswamy et al.* [2001] the trend increases from the Southern to the Northern Hemisphere. A fairly symmetric pattern of temperature change, with a relative minimum at the equator, was also found in a GCM simulation with imposed ozone depletion and increase in carbon dioxide [*Langematz et al.*, 2003]. The midlatitude maxima in the simulated temperature change are consistent with larger ozone depletion at midlatitudes (Figure 1, top left) from homogeneous chemistry. The recent review of model simulated temperature trends by *Shine et al.* [2003] indicates that both ozone and carbon dioxide contribute to the global cooling of the upper stratosphere.

[17] In the lower polar stratosphere, temperature changes due to ozone depletion from heterogeneous chemistry in our model can be larger than in a model without interactive chemistry (where the ozone change is imposed; see, for instance, *Langematz* [2000]), because we take into account the feedback of the temperature change on the ozone chemistry [*Steil et al.*, 2003]. In this respect, our results are consistent with those of *Austin* [2002]. In the southern polar lower stratosphere, the −4 K change in the annual mean is consistent with the trend from Figure 5b of *Ramaswamy et al.* [2001]. In the mesosphere, the 2000–1960 temperature change decrease with height. The cooling in the mesosphere can be explained by both the increase in carbon dioxide and ozone depletion. For reference, Figure 1 (middle right) shows the annual, zonal mean temperature from the 20-year average from the 1960 simulations. The typical features are seen, such as the very cold equatorial tropopause, asymmetry at the poles, with the southern polar temperature 10 K colder, and the warm stratopause.

[18] There is a general increase of water vapor throughout the atmosphere from the 1960 to the 2000 simulations (Figure 1, bottom left). The change in water is statistically significant at the 99% level almost everywhere. In the troposphere the increase is related to the positive temperature change due to the increase in greenhouse gases and in the middle atmosphere from the increase in methane, and possibly transport from the troposphere. Figure 1 also shows negative changes of water vapor in the lowermost equatorial stratosphere and the positive changes above. Qualitatively similar changes have been found in HALOE observations from 1992 to 2001, but lack a fundamental understanding [*Rosenlof*, 2002]. In the region that is important for ozone chemistry (100–50 hPa), increased dehydration (by settling of ice particles) occurs only at the South Pole. In this latter case, the increased dehydration can be

considered to be a feedback from the lower temperature in the 2000 simulation due to ozone depletion (see Figure 11). The prevalent increase of water vapor by 12% in the middle atmosphere in four decades is considerably less than what is suggested by recent estimates of water vapor increases, that are however still awaiting an explanation [*Rosenlof et al.*, 2001]. Given that methane is oxidized to water vapor (H_2O + $2CH_4$ approximately constant), from the imposed change in the methane mixing ratio at the surface (0.5 ppmv) one would expect a water vapor change of 1 ppmv. While the simulated absolute water vapor change estimated from Figure 1 is typically between 0.6 and 0.7 ppmv. This bias is most likely caused by deficiencies in the representation of processes in the thin tropopause layer that separates the moist troposphere from the dry stratosphere. Relevant processes for water in the tropopause layer are most likely small scale and difficult to represent in GCMs. Further there is also a lack of general understanding of the processes and trends in this region. It is for example not understood why water vapor may increase in the middle atmosphere while the tropical tropopause temperature and water vapor just above it decreases [*Rosenlof*, 2002]. Therefore modeled water vapor changes are not in the focus of this work. For reference, the 1960 water vapor field as simulated by the model is shown (Figure 1, bottom right). Note the asymmetry in the polar distributions (slightly more downward and poleward extension of the 5 ppmv contour), indicating more water vapor in the northern polar stratosphere, because of the stronger residual circulation and mixing there (see, for instance, Figures 8 and 12), and consistent with the average temperature difference between the hemisphere shown before.

4. Changes in Total Ozone and in the Vertical Distribution of Polar Ozone

[19] The 20-year average of the total ozone from the 1960 simulation is shown in Figure 2 (upper right) together with TOMS satellite observations data for 1979 (upper left). The latter is here considered to represent almost unperturbed conditions, prior to the occurrence of ozone depletion. The comparison with the TOMS satellite observation data shows that the model reproduces the seasonal and latitudinal variations. Note for instance the broad maximum in total ozone during Northern Hemisphere spring, extending from the North Pole to 60°N and the midlatitude total ozone maximum during the Southern Hemisphere spring. However, the calculated total ozone is biased high by about 10% with the largest deviations at middle latitudes and tropics. As discussed in part 1, the high bias in total ozone is due to an overestimate of stratosphere to troposphere transport related to numerical deficiencies in the transport scheme. If only total stratospheric ozone above 90 hPa is considered, the differences are much smaller (Figure 3 of part 1). Of interest in Figure 2 is that at the South Pole the calculated total ozone for the 1960 simulation remains roughly constant through the winter and increases from the winter to spring, which is a typical seasonal behavior for pre-ozone hole conditions of the atmospheric composition [*Dobson*, 1968; *Brasseur and Solomon*, 1986].

[20] The total ozone change from pre-ozone hole conditions (e.g., 1979) to the present time as illustrated by the TOMS observations here presented in Figure 2 (left, middle and bottom panels) is characterized by substantial ozone depletion during the Antarctic spring (up to 45–50% decrease) and relatively weaker depletion during the Arctic spring (at most 15% decrease). In the summer, the change in TOMS total ozone is also negative, at most 5% in the Arctic and 10% in the Antarctic. These features in total ozone are well known [*Solomon*, 1999; *Fioletov et al.*, 2002]. The results from our simulations (right, middle and bottom panels) show that the 2000–1960 change in total ozone includes all the important features in total ozone changes reported for the TOMS observations, as the formation of the Antarctic ozone hole and the ozone depletion up to about 15% in Arctic spring. In the model the lowest total ozone in Antarctica occurs about 2 weeks later than in observations. Given that the speed of ozone destruction is proportional to ClO*ClO and not O_3, the high bias in lower stratospheric ozone reported before (see part 1) causes a time shift in the occurrence of the lowest total ozone. The delayed recovery is associated with the model cold bias at the South Pole in the upper stratosphere (see the model intercomparison of *Austin et al.* [2003] and Figure 19). Importantly, the simulated large polar ozone depletions are seasonally limited, so that during the summer the total ozone decrease is limited to 5% to 10% decreases in the Arctic and Antarctic, respectively, as observed. These features are also found for the 1990–1960 change, except for the localized and large Arctic ozone depletion in March and April.

[21] At 80°N, the seasonal cycle of the vertical distribution of the relative ozone change between the 1990 and 1960 simulations is compared to the change between the 2000 and 1960 simulations in Figure 3. Clearly, the larger decrease reported for the 2000–1960 total ozone change during March and April is due to ozone depletion in the lower stratosphere (about 20% in average), highlighting the role of non-linear effects in the ozone depletion by heterogeneous chemistry, which for cold conditions is dominated by the ClO quadratic catalytic cycle involving the Cl_2O_2 dimer (*Molina and Molina* [1987]; for a review, *Solomon* [1999]). This implies that the 10% increase in total chlorine between the 1990 and 2000 simulations corresponds to about a 20% increase in destruction rate. Around 80 hPa the severest ozone decrease in March and April 2000 is twice that in 1990 (with respect to 1960, see also Figure 6). Here the effect of chlorine increase is amplified by a calculated cooling (see section 5.1 and Figure 5). In the upper stratosphere instead, the 2000–1960 and 1990–1960 changes are very similar, as expected from ozone depletion from homogeneous chlorine chemistry, linear in chlorine.

[22] At 80°S, results are shown only for the 2000–1960 change. The vertical profile of the relative ozone change is dominated by the heterogeneous ozone destruction from September to November in the lower stratosphere. The ozone poor region slowly propagates downward during the southern spring. Locally, decreases can be larger than 90%, see section 6, than for zonal and monthly averages. For Antarctica the 1990 and 2000 simulations are rather similar, expect for a faster depletion in September in the ozone hole region in 2000.

[23] Note the positive changes during the late spring and summer between 30–10 hPa in Figure 3. These changes are due to a chemical compensation effect (less ozone above

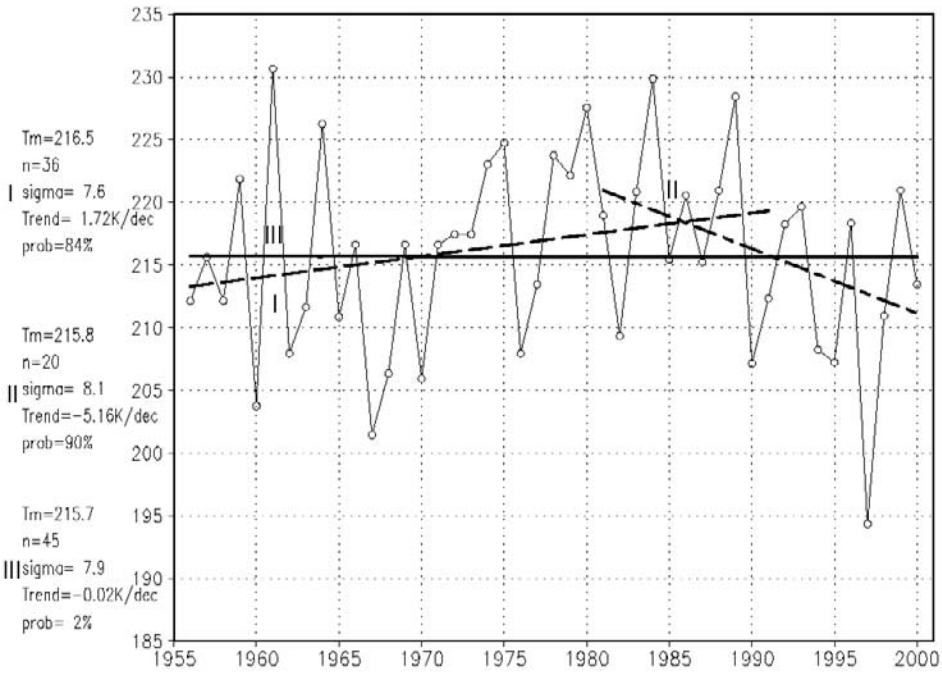

Figure 4. March mean temperature at the North Pole at 30 hPa from the Freie Universität Berlin analyses from 1955 to 2000. Trend I includes data from 1955 to 1991; Trend II from 1981 to 2000; and Trend III from 1955 to 2000; statistical significances are added to the left side.

facilitate the ozone formation below from molecular oxygen) and could also at least in part be due to increased downward motion, as shown in the section 5.1.

5. Temperature Changes and Dynamical Feedback

5.1. Arctic Middle Atmosphere

[24] Figure 4 shows the monthly mean 30 hPa North Pole temperature in March from the Freie Universität Berlin (FUB) analyses from 1955 to 2000 (update from *Labitzke and van Loon* [1994]). As pointed out by *Labitzke and van Loon* [1994], the North Pole temperature is characterized by large year-to-year variability and also longer timescale variations from 1955 to the present time. Therefore, if the full 1955 to 2000 time series is considered, the North Pole temperature does not show a trend. While if shorter time series are considered, trends may become apparent. For instance a warming trend from the 1960s to the late 1980s and a cooling trend during the last 20 years. The longer timescale variations in the polar temperature have been reported also from other sources, for example, NCEP reanalysis [*Waugh et al.*, 1999]. The question of interest is if ozone depletion and increase in greenhouse gases are currently perturbing the atmosphere enough to influence the North Pole temperature variations of the 1990s with respect to the 1960s. Note that very similar variations are found for the March temperature at 80°N from the FUB analyses. Here the North Pole record is shown because it ranges from 1955 to present, while the record at 80°N ranges only from 1965 to present.

[25] The evolution at 80°N of the monthly zonal mean temperature changes between the 1960 and 1990 simulations and between the 1960 and 2000 simulations are shown in Figure 5. The time series is shown, from July to June. The grey shading indicates statistically significant differences (95% and 99% levels, t-test). The reference (bottom panel of Figure 5) is the 20-year mean of the monthly zonal mean temperature for the 1960 simulation. Major features in the 1960 temperature are the seasonal evolution of the stratopause (~1 hPa; 250 to 280 K) lower and warmer during summer, very cold (~170 K) summer upper mesosphere, lower stratosphere temperature minimum (~200 K) in winter, and surface warming in summer. These features compare well with observations [*Fleming et al.*, 1990].

[26] The 1990–1960 change is characterized by a general cooling of the middle atmosphere and weak warming of the surface layer and/or troposphere. In summer and early autumn, the negative and significant change is largest at the stratopause (−5 to −6 K), as for the annual, zonal mean temperature change (Figure 1). During the winter months the pattern of change is complicated. In December, there is a weak (1 K) warming in the lower and middle stratosphere and a strong cooling in the mesosphere. The latter descends, and intensifies slightly, to the upper stratosphere in January and is a response to the December warming. During spring, the upper stratosphere is characterized by weak cooling and the lower stratosphere by weak warming. The December warming is due to the occurrence of a few exceptional sudden stratospheric warmings early in the season in the 1990 simulation (not shown). Interestingly, the unusual early occurrence of such events is only observed within the last 15 years [*Naujokat et al.*, 2002].

[27] During the northern summer, lower temperatures characterize the 2000 simulation with respect to the 1960 simulation, the cooling (−6 to −7 K) at the stratopause being

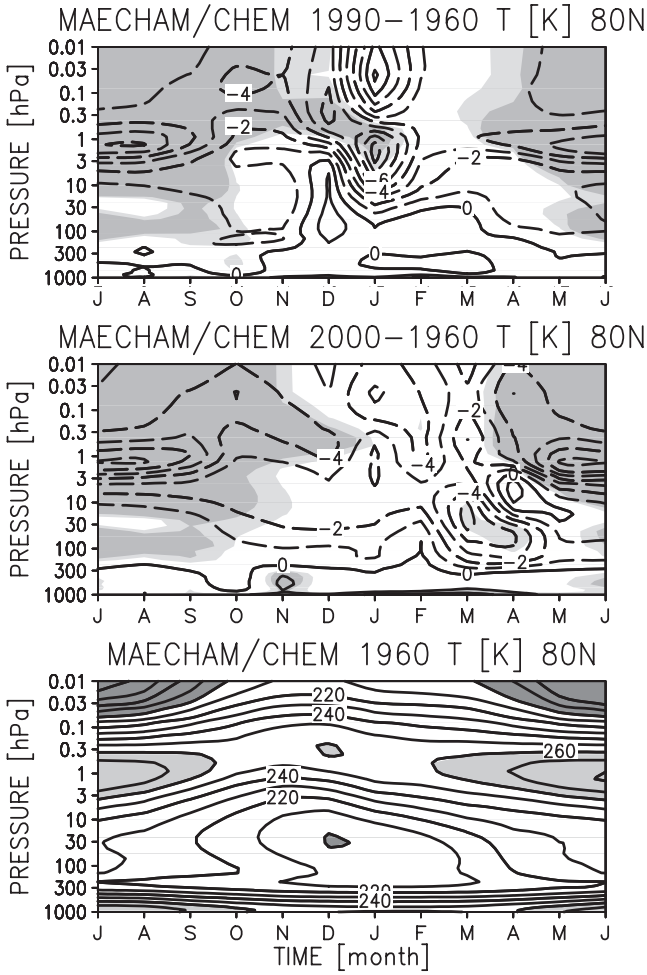

Figure 5. Monthly, zonal mean temperature at 80°N. Difference (top) between the 20-year averages of the 1960 and 1990 simulations, 1990–1960; (middle) the 20-year averages of the 1960 and 2000 simulations, 2000–1960. Contour: 1 K. Dark (light) shades denote significance at 99% (95%) level. (Bottom) 20-year averages from the 1960 simulation. Contour: 10 K, light shade > 260 K, dark shade < 200 K.

just slightly larger than that found for 1990–1960, consistently with a slightly more perturbed atmosphere. In the lower stratosphere the 2000–1960 change for the months of March and April is characterized by a pronounced cooling (−4 to −5 K), statistically significant at the 95% level. The temperature difference is no longer significant in the upper stratosphere in March, where the interannual variability in the model is larger. On average, in April a slight warming (1 K) appears in the upper stratosphere.

[28] Another view of the difference in the temperature and ozone changes, 1990–1960 and 2000–1960 respectively, is given in Figure 6, where their respective changes in March zonal mean temperature and percentage ozone are shown. Concerning ozone, the relative change is similar for 1990–1960 and 2000–1960 in the mesosphere, upper stratosphere and southern polar stratosphere. In the northern polar stratosphere instead, the 2000–1960 relative change reaches −20%, about twice that for the 1990–1960 change. Concerning the temperature, the middle atmosphere in general is about one degree colder in 2000 than in 1990. The major difference between the 1990–1960 and 2000–1960 changes is again found in the Arctic middle atmosphere: while the lower stratosphere is warmer in the 1990 simulation with respect to the 1960 simulation, it is up to 6 K colder in the 2000 simulation with respect to the 1960 simulation. Above, in the mesosphere, respective opposite changes are found, as a results of changed dynamics.

[29] The 2000–1960 cooling in March is consistent with the variations shown from the FUB analyses in Figure 4, given that the early 1960s are on average warmer than the late 1990s (as it can be seen visually in Figure 4, by excluding the even warmer 1980s). The 1990–1960 March warming from our simulations is also consistent with the warming trend from the early 1960s to the late 1980s seen in the FUB analysis in Figure 4. Note also that the significant difference in March temperature occurring in 2000–1960 would appear very similarly in the difference 2000–1990, because the respective change 1990–1960 is small. The March cooling of the lower stratosphere during the last decade is observed [*Ramaswamy et al.*, 2001; *Randel and Wu*, 1999a] and indeed is also found from the FUB analysis used in Figure 4 and in part 1.

[30] In order to interpret the temperature changes among the three simulations, Figure 7 shows the seasonal cycle of the average vertical component of the EP-flux [*Andrews et al.*, 1987] for the 1960, 1990, and 2000 simulations at 100 and 300 hPa. The vertical EP-flux is a measure of the dynamical forcing provided by tropospheric meteorological eddy activity to the stratosphere, and it is related to the eddy heat flux [*Andrews et al.*, 1987]. The vertical EP-flux changes among the simulations are generally small; the point here is to search for consistency with the temperature changes. For instance, in December the average EP-flux of the 1990 simulation is the largest at both levels, in agreement with the temperature changes in Figure 5. Concerning the temperature in March, influenced by the January and February eddy activity [*Newman et al.*, 2001], it is of interest to note that the January–February EP-fluxes are virtually the same for the 1960 and 2000 simulations, although the March temperatures are not. Therefore other factors should contribute to the 2000–1960 temperature change in March in the model, namely the occurrence of ozone depletion and increase in greenhouse gases in the 2000 simulation, both acting in the direction of cooling the lower polar stratosphere. In March 2000, the 100 hPa EP-flux is smaller than in 1960, and is interpreted as a response to the cooling, as discussed below and in section 7. Support to this interpretation is the fact that the 300 hPa March EP-fluxes are the same for all simulations. With respect to the 1960 EP-flux, the 1990 EP-flux is smaller in January and larger in February. The latter favors a warming of the lower polar stratosphere and can therefore mask any effect from ozone depletion and increase in greenhouse gases. There might be also an influence of the SST on the vertical EP-fluxes and therefore average North Pole temperature in the lower stratosphere. The mechanism involved in such a link is not in the focus of this work, it will be addressed in a later study.

[31] The linkage between changes in zonal mean zonal wind and changes in wave effects, and vice versa, is shown

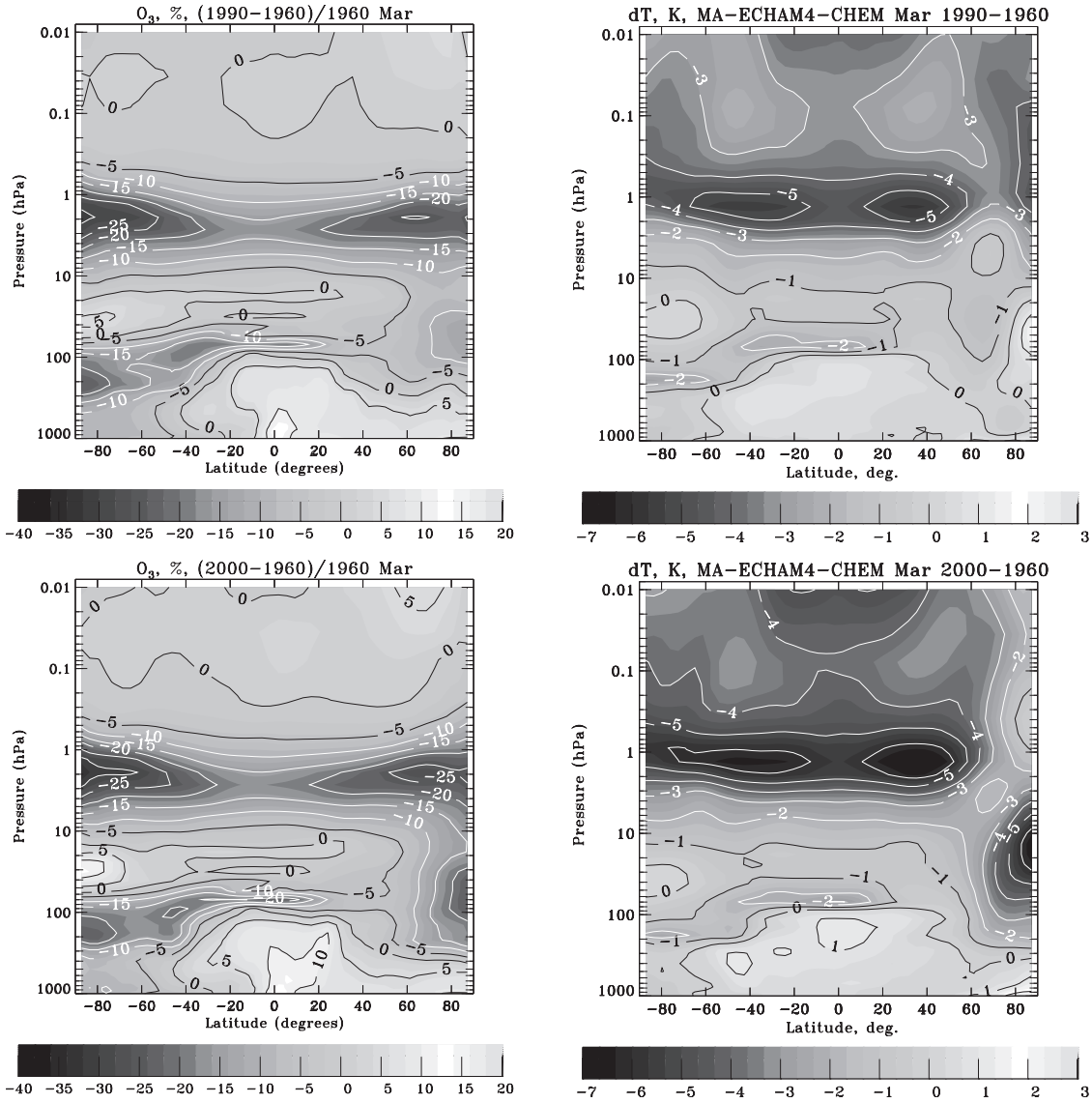

Figure 6. Difference of (left) March zonal mean ozone and of (right) March zonal mean temperature: (top) between the 20-year averages of the 1960 and 1990 simulations, 1990–1960; (bottom) the 20-year averages of the 1960 and 2000 simulations, 2000–1960. Contours: (left) 5%; (right) 1 K.

by means of the change in residual vertical velocity in the polar cap (Figures 8 and 9). As explained by theory [*Andrews et al.*, 1987], the residual vertical velocity depends on wave dissipation and breaking, itself influenced by the zonal mean zonal wind. In turn, wave dissipation and breaking provide momentum forcing and change the zonal mean zonal winds. The residual vertical velocity, area weighted average poleward of 60°N and its change is shown in Figures 8 and 9. The 2000–1960 zonal mean zonal wind change and the 1960 reference are shown in Figure 10. Given that a cooling of the arctic lower stratosphere in spring is found only for the 2000 simulation, the attention is restricted to the 2000–1960 changes. The time series is shown from July to June. The 1960 reference (Figure 8, bottom) shows that downwelling (negative) occurs in the polar middle atmosphere from autumn to early spring. The downwelling is strongest in January, ranging from −0.5 to −2 mm/s in the stratosphere to −10 mm/s in the mesosphere. Upwelling (positive) is present instead during summer, more clearly in the mesosphere where it reaches 20 mm/s in June and July.

[32] In the upper mesosphere the 2000–1960 change in residual vertical velocity indicates that the circulation tends to decrease (e.g., both summer upwelling and winter downwelling are reduced, by about 10%). In the stratosphere changes are generally small or display somewhat complicated patterns. During winter there is a tendency for an increase in downwelling in the upper stratosphere and lower mesosphere. At the time of the March cooling reported before, downwelling is reduced between 100 and 3 hPa, and increased above. The increase is largest in the lower mesosphere ($\sim$1 mms^{-1}, see also Figure 9, left), about 20% (or more) of the 1960 average downwelling. These changes in downwelling indicate that in March there is decrease in dynamical heating and decrease ozone transport from above in the lower stratosphere, where the

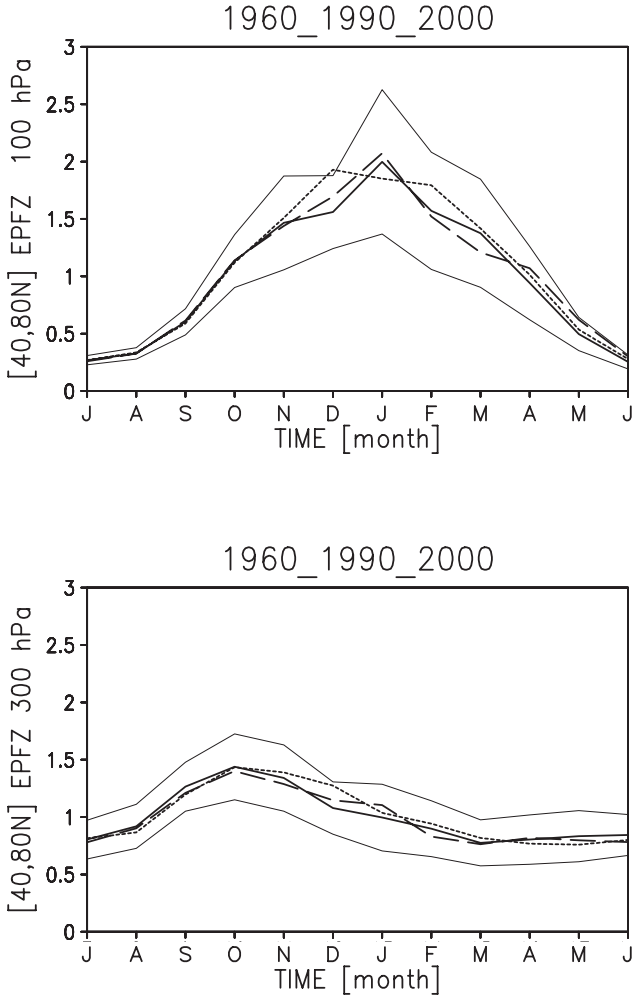

Figure 7. Monthly mean vertical component of the EP-flux (40°–80°N area weighted average), normalized with respect to the 20-year 1960 annual average. 20-year average from the 1960 simulation (dark solid curve), the 1990 simulation (short-dashed curve), and the 2000 simulation (long-dashed curve). The two light solid curves are the envelope of ±1 standard deviation from the 1960 simulation. (top) At 100 hPa and (bottom) at 300 hPa.

temperature change is negative and ozone depletion occurs. Therefore dynamical effects can reinforce the cooling. On the contrary, above the region of cooling, dynamical effects in the model tend to oppose it, by reinforcing the downward motion and associated dynamical heating. Thereafter, in April the increase in downwelling is shifted downward to the stratosphere. These results are consistent with the decrease in the magnitude of the cooling above 10 hPa in March and the weak warming in April in the upper stratosphere.

[33] *Newman et al.* [2001] suggest a sensitivity of 1.7 K per 10% change in dynamical forcing. By comparing the average midwinter mean temperature and residual vertical velocity in the Northern and Southern Hemisphere in the 1960 simulation in the polar lower stratosphere, the estimate of the temperature sensitivity to dynamical forcing that can be drawn from the MAECHAM4/CHEM model is comparable to that of *Newman et al.* [2001]: at ~30 hPa, an increase by a factor 2 in the residual vertical velocity (Figures 8 and 12, bottom panels) correspond to a ~20 K difference (Figures 5 and 11, bottoms). The reduced downwelling (30–10 hPa) in March is about 20%; therefore it could contribute a few degrees to the local cooling. However, it may not last enough in time to really affect the average temperature, given that in April the downwelling is instead slightly increased.

[34] To investigate which eddies are involved in the reported changes in downwelling, the residual vertical velocity due to planetary waves has been computed from the Eliassen-Palm (EP) divergence following the downward control principle [*Haynes et al.*, 1991; *Andrews et al.*, 1987]. The difference between the residual vertical velocity computed from the model variables and that from the EP divergence is thereafter dominated by the contribution from gravity waves (e.g., the parameterized component). The

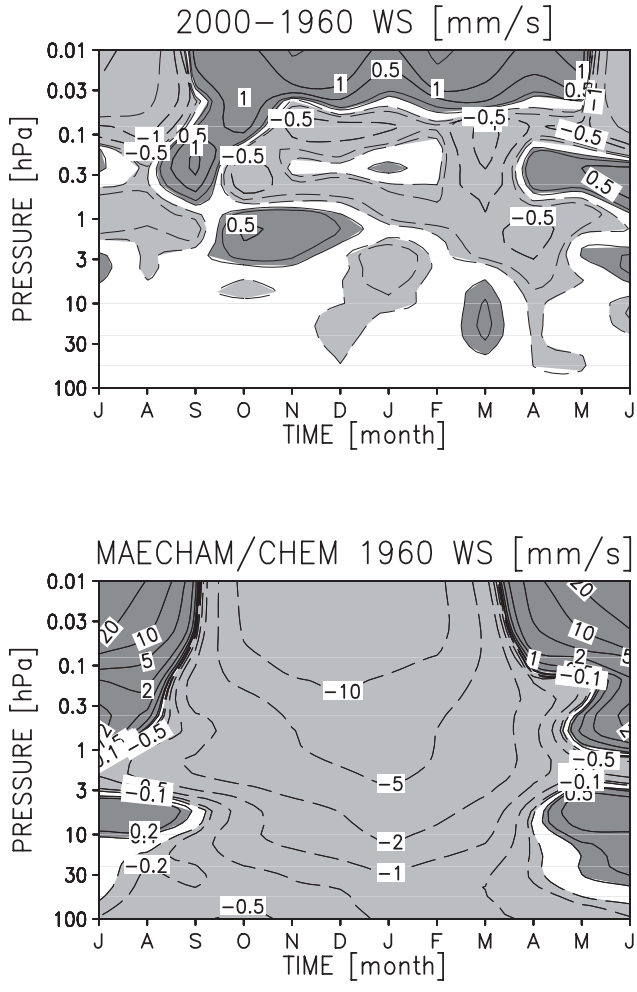

Figure 8. Monthly mean of the residual vertical velocity, area weighted average poleward of 60°N. (top) Difference between the 20-year averages of the 1960 and 2000 simulations, 2000–1960. (bottom) 20-year averages from the 1960 simulation. Contours: ±0.1, ±0.2, ±0.5, ±1, ±2, ±5, ±10, ±20, ±50 mms^{-1}; positive (negative) values are dark (light) shaded.

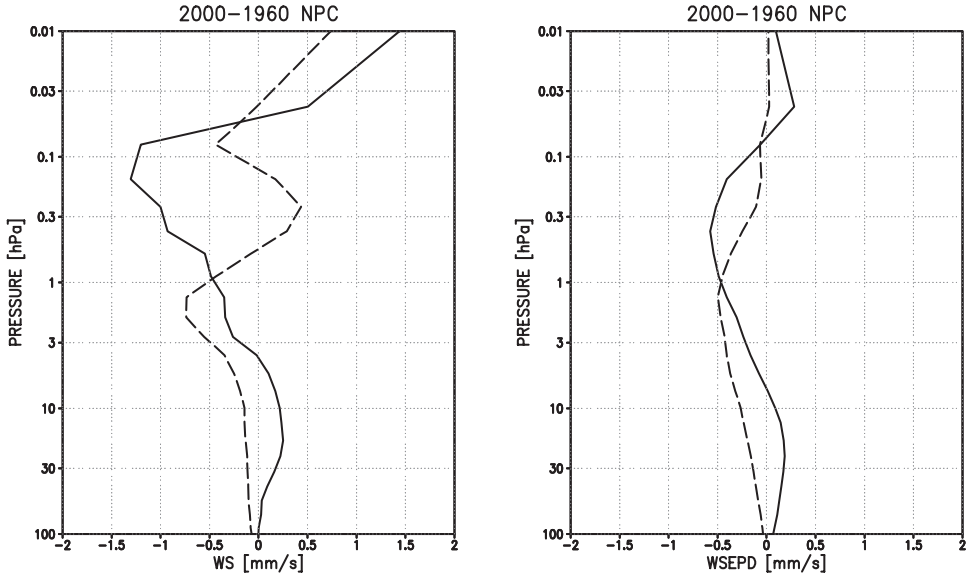

Figure 9. Vertical profile of March (solid curve) and April (dashed curve) residual vertical velocity, area weighted average poleward of 60°N, difference between the 20-year averages of the 1960 and 2000 simulations, 2000−1960. (left) From Figure 7; (right) from the EP divergence only. Unit: mms^{-1}.

vertical profile for the March (solid) and April (dashed) change in the residual vertical velocity from downward control is shown in Figure 9 (at right, the profile at left is from Figure 8). In the mesosphere in March the contribution to the increased downwelling from the planetary waves is smaller than the total one, less than 1/3 at 0.1 hPa (where the negative difference is largest). The difference in residual velocity in the mesosphere therefore appears to be dominated by the response of the gravity wave induced forcing. In the lower to middle stratosphere (100−10 hPa), the contribution from the planetary waves alone instead can account for most of the decrease in the downwelling associated with the March cooling. The planetary waves also appear to be responsible for the downward shift of the negative difference from March to April, accounting for most of the difference in April in the upper stratosphere.

[35] A plausible reason for the increase in the gravity wave induced downward motion (indirect diagnostics of increased gravity wave momentum flux deposition in the lower mesosphere) is found in the increase in stratospheric zonal winds associated with the lower stratospheric cooling (Figure 10). The stronger westerlies in the stratosphere (in March, ∼6 m/s difference) imply enhanced filtering (removal) of eastward gravity waves (while westward waves propagate freely upward) and therefore a net gravity wave momentum flux at the stratopause that is more negative than in the case of weak westerlies. In turn, a more negative net gravity wave momentum flux allows for stronger deceleration of the westerlies in the mesosphere. Figure 10 shows that the zonal winds are indeed weaker in the mesosphere in 2000, from January to summer. This behavior is a typical response of gravity waves propagating in a changing background wind (see, for instance, the analysis of a similar situation, albeit due to different causes, given by *Manzini and McFarlane* [1998]). Note that the specification of the gravity wave sources is not changed in the simulations. Therefore only a redistribution of the gravity wave induced

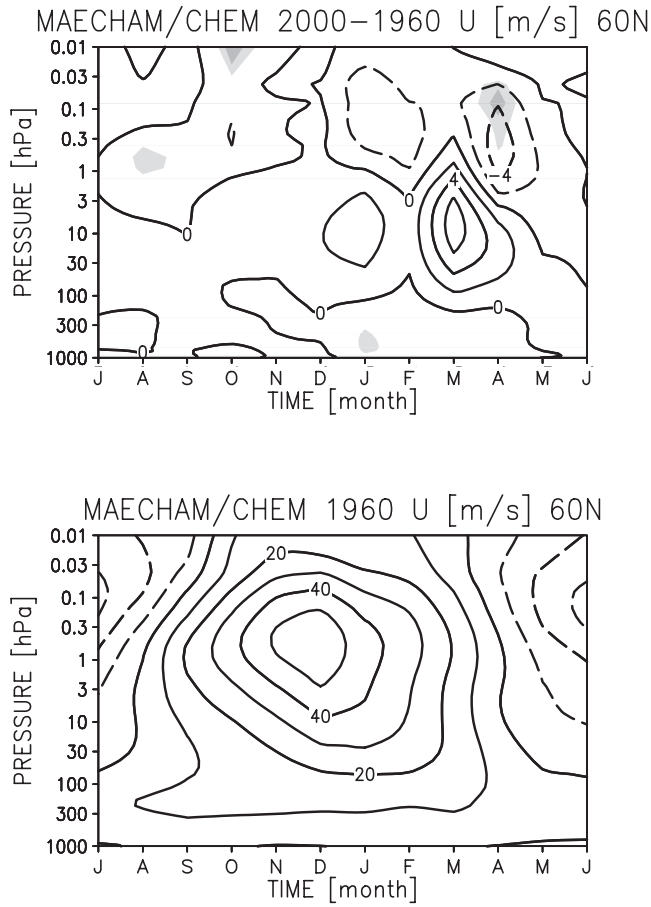

Figure 10. Monthly, zonal mean zonal wind at 60°N. Difference (top) between the 20-year averages of the 1960 and 2000 simulations, 2000−1960. Contour: 2 ms^{-1}. Dark (light) shades denote significance at 99% (95%) level. (bottom) 20-year averages from the 1960 simulation. Contour: 10 ms^{-1}.

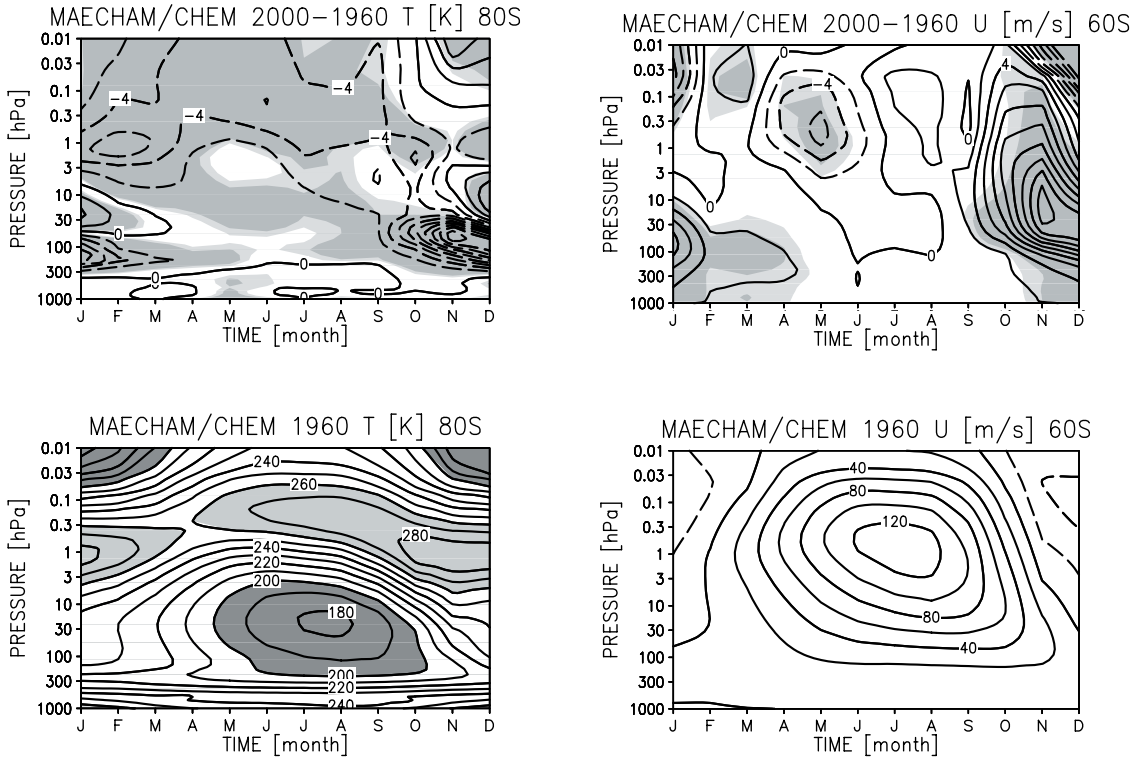

Figure 11. Monthly, zonal mean (left) temperature at 80°S and (right) zonal wind at 60°S. (top) Difference between the 20-year averages of the 1960 and 2000 simulations, 2000–1960. (bottom) 20-year averages from the 1960 simulation. Contours: (top left) 2 K. Dark (light) shade denote significance at 99% (95%) level. (bottom left) 10 K, light shade > 260 K, dark shade < 200 K; (top right) 2 ms^{-1}. Dark (light) shades denote significance at 99% (95%) level. (bottom right) 20 ms^{-1}.

forcing occurs, as the decrease in downwelling (just above the increase) in the upper mesosphere shows. The change in Figure 10 also shows that the polar vortex is stronger and lasts longer in the 2000 simulation (with respect to the 1960) in the lower stratosphere in March and April, as expected by the change in the mean temperature. The zonal wind changes are not statistically significant, giving evidence of the large interannual variability occurring in the model, a realistic feature.

[36] Figure 9 also shows that the downwelling in the upper stratosphere and lower mesosphere contributed by the planetary waves increased from 1960 to 2000. A plausible cause is the reported changes in zonal winds in the mesosphere that might increase planetary wave dissipation. Note that in the lower mesosphere, the largest negative changes in zonal wind occur in April (Figure 10), so that the vertical wind shear around the stratopause is increased in April, facilitating dissipation. Planetary waves can also be dissipated by gravity wave breaking, which is estimated to be increased. From March to April, the change in downwelling contributed by the planetary waves is shifted downward, in agreement with the downward shift of the negative changes in zonal wind seen in Figure 10.

5.2. Antarctic Middle Atmosphere

[37] The evolution at 80°S of the monthly zonal mean temperature and zonal mean changes between the 1960 and 2000 simulations are shown in Figure 11. The time series is shown, from January to December. The shading indicates statistically significant differences (95% and 99% levels, t-test). The reference (bottom panels) is the 20-year mean for the 1960 simulation. In the Antarctic, the 1960 temperature extrema are more pronounced than in the Arctic (Figure 5). For instance, the Antarctic stratopause temperature is 270–280 K and the Antarctic winter lower stratosphere temperature is 180 K (compare with Figure 5). Consistently, much stronger westerlies characterize the Antarctic in winter (compare with Figure 10). Note that although the contrast in temperature extrema between the Arctic and Antarctic polar latitudes is a realistic feature, it is exacerbated in the model by the cold bias in the upper stratosphere, largest during southern winter. For a discussion of the cold bias in middle atmosphere models, see *Pawson et al.* [2000] and *Austin et al.* [2003]. For an evaluation of the cold bias in the MAECHAM4 model, see *Manzini and McFarlane* [1998].

[38] The most distinct 2000–1960 change is the strong cooling in the spring and summer of the lower stratosphere, statistically significant at the 99% level. The temperature change is largest in November at ~70 hPa and is clearly a consequence of the development of the ozone hole in the 2000 simulation. The area of large negative differences is limited in depth, the change being substantially reduced above 30 hPa. In the mesosphere (November–December) and in the middle to lower stratosphere (November–February) the temperature change is positive.

[39] Evidence of a warming above the lower stratospheric cooling in November–December is reported from Antarctic radiosonde stations (30 hPa, uppermost level) and in the

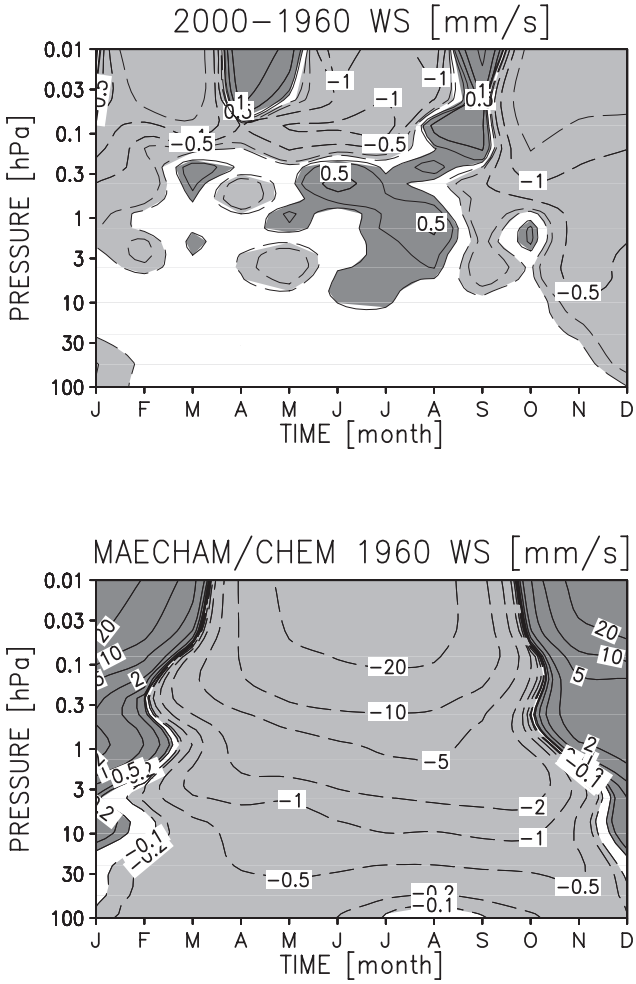

Figure 12. Monthly mean of the residual vertical velocity, area weighted average poleward of 60°S. (top) Difference between the 20-year averages of the 1960 and 2000 simulations, 2000−1960. (bottom) 20-year averages from the 1960 simulation. Contours: ±0.1, ±0.2, ±0.5, ±1, ±2, ±5, ±10, ±20, ±50 mms^{-1}; positive (negative) values are dark (light) shaded.

NCEP reanalysis [*Randel and Wu*, 1999a]. It has also been simulated previously by *Mahlman et al.* [1994] in a simulation over a few years with simplified ozone depletion chemistry with the SKYHI model, as well as in the work of *Austin* [2002]. A dynamical heating concurrent to an imposed ozone hole in a short simulation with a GCM was also found by *Kiehl et al.* [1988] and was indeed used as an argument not in support of a dynamical origin of the ozone hole at the time.

[40] *Mahlman et al.* [1994] attributed the warming to changes in the residual circulation because it was too large to be accounted for solely by radiative processes. By computing the residual vertical velocity, we find that indeed in November in the stratosphere the downwelling is increased. In October it is increased only in the mesosphere (Figure 12). The planetary wave contribution to the increase in downwelling (Figure 13, right) is small in the mesosphere, where gravity waves contribute most of the change in the increased downward motion (the total is about four times larger than the planetary wave contribution in this case). The downward shift from October to November in the change in the residual vertical velocity in the stratosphere is instead mostly contributed by the planetary waves. The change in the stratospheric winds (statistically significant at the 99% level, Figure 11) is considered to be responsible for the increase in the gravity wave induced forcing of the circulation, hence larger downwelling in the mesosphere. Above the stronger stratospheric westerlies, easterlies appear (or are reinforced) in the mesosphere in the 2000−1960 change in zonal wind shown in Figure 11. In the lower stratosphere, the stronger westerlies in the 2000 simulation (with respect to the 1960 simulation) indicate that the polar vortex is stronger and lasts longer in the 2000 simulation.

[41] The reference in Figure 12 is the 20-year mean of the monthly residual vertical velocity, average southward of 60°S from the 1960 simulation. In the lower and middle stratosphere the winter downwelling is weaker than in the Arctic, as expected because of the weaker forcing from planetary waves. In the mesosphere instead, the winter downwelling is stronger (factor 2) than in the Arctic, another manifestation of the sensitivity of the gravity wave induced driving of the circulation in the mesosphere to the stratospheric winds.

6. Chlorine Partitioning, Ozone Depletion, and Polar Stratospheric Clouds

[42] To illustrate the behavior of chlorine compounds and their role in polar ozone depletion, we focus in this section on snapshots of typically cold days in spring at 70 hPa (Figures 14 and 15). The simulations are characterized by relatively large (and realistic) interannual and daily variability. The cold days in Figures 14 and 15 are somewhat extreme cases and not average conditions. Note also that snapshots are shown because heterogeneous chemistry for active chlorine is strongly non-linear and averages or time series at a fixed location would mix up processes inside and outside the polar vortex (for a temporal behavior on idealized trajectories inside the vortex with the same chemistry, see *Brühl et al.* [1998]). In the figures the vortex coincides approximately with the region near the pole where temperatures are below 205 K.

[43] Concerning the Arctic lower stratosphere, Figure 14 shows that inside the vortex, chlorine is activated, by heterogeneous chemistry on NAT-PSCs, for both the 1960 and 2000 examples. However, the area where chlorine is activated is larger and the amount of ClO_X (ClO_X = ClO + $2Cl_2O_2$ + $2Cl_2$ + ClOH + Cl, reactive chlorine) is from four times to an order of magnitude more in 2000 than in 1960. Note that total organic chlorine in 2000 is more than 4 times as much as in 1960 (Table 1), a ratio also approximately valid for inorganic chlorine in the lower stratosphere. Clearly, in the 2000 example the peak in ClO_X corresponds to considerable ozone depletion (pool of high ClO_X and low O_3 in the eastern Arctic, where also the temperature minimum is located). It is not so for the 1960 simulation, although the 1960 minimum temperature on the shown day is below the existence temperature for NAT-PSCs. The relative fraction of the reservoir $ClONO_2$ in inorganic chlorine is larger in 1960 because of less de-nitrification

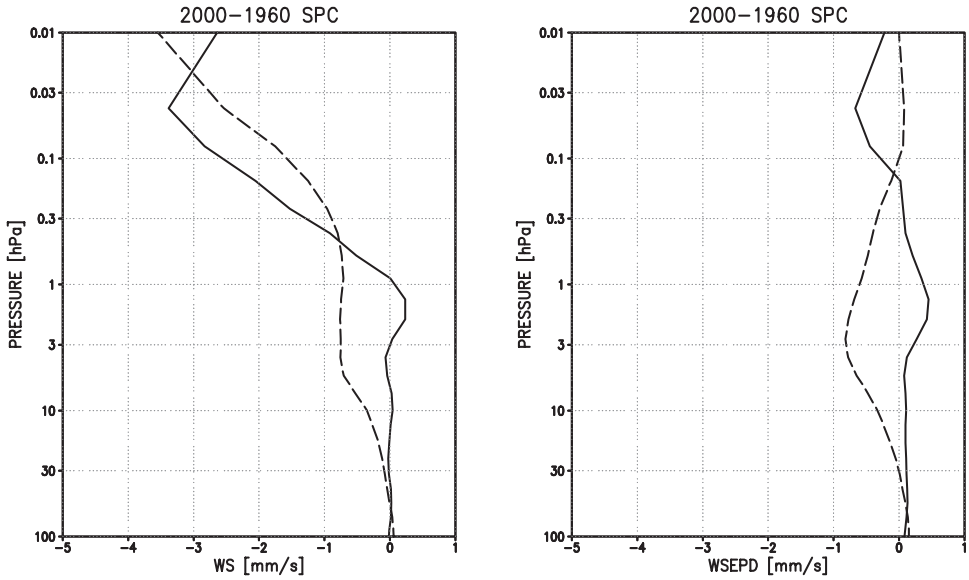

Figure 13. Vertical profile of October (solid) and November (dashed) residual vertical velocity, area weighted average poleward of 60°S, difference between the 20-year averages of the 1960 and 2000 simulations, 2000−1960. (left) From Figure 11; (right) from the EP divergence only. Unit: mms^{-1}.

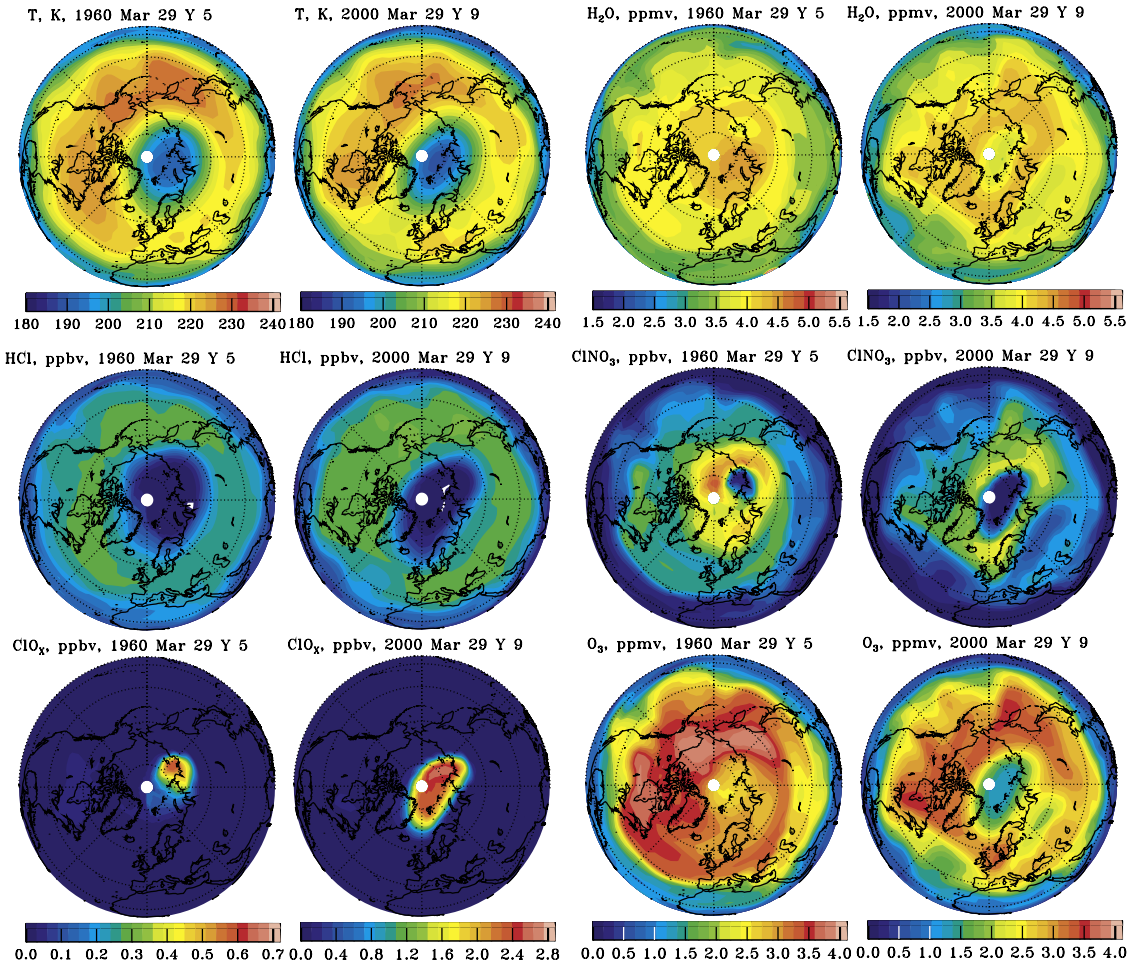

Figure 14. March snapshots at 70 hPa of temperature (K), water vapor (ppmv), chlorine species (ppbv) and ozone (ppmv) for the Arctic, cold years. First and third columns: selected example from the 1960 simulation. Second and fourth columns: selected example from the 2000 simulation. Note that for the chlorine species, the 1960 color bar ranges from 0 to 0.7 ppbv, while the 2000 color bar ranges from 0 to 2.8 ppbv.

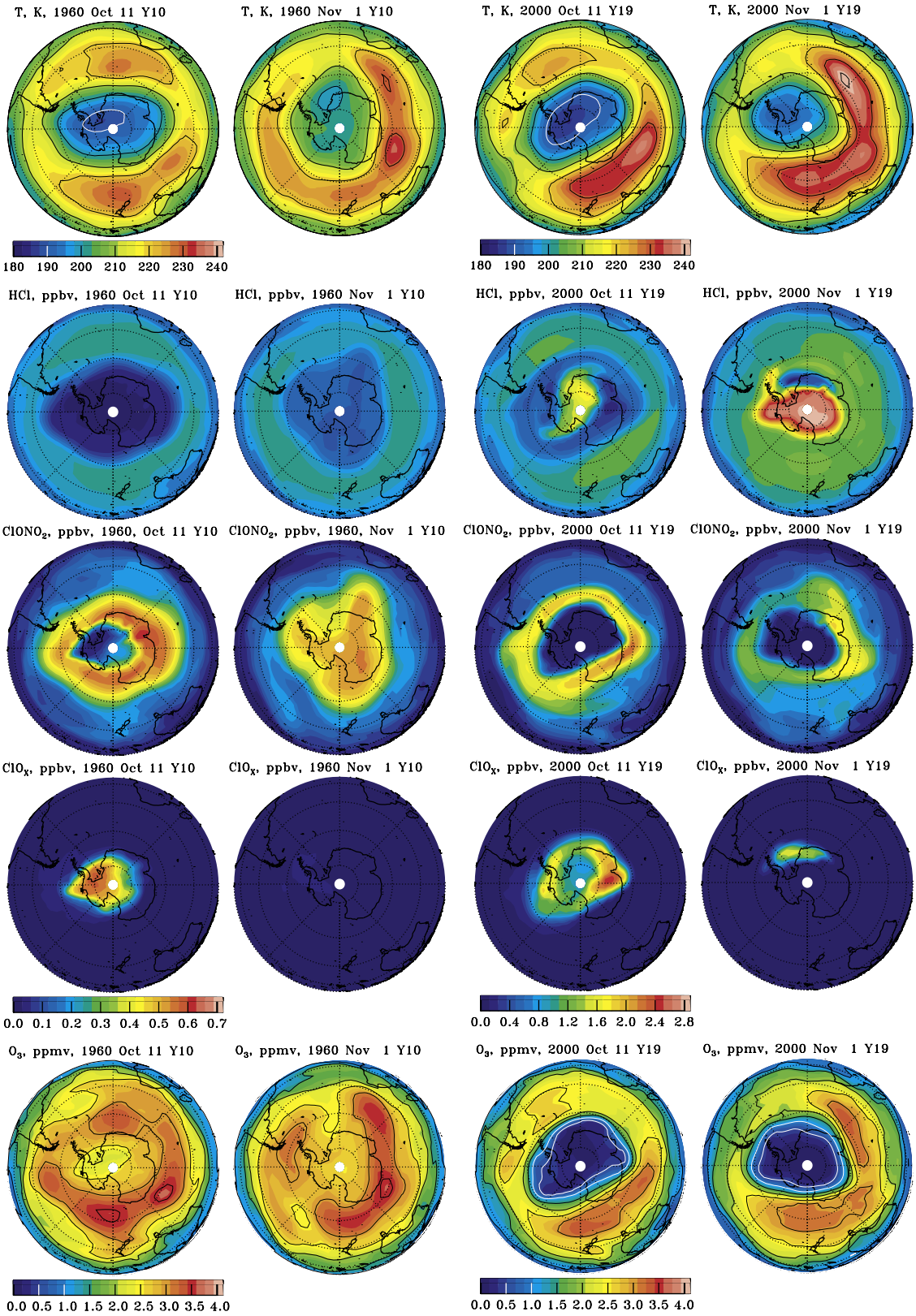

Figure 15. October (first and third columns) and November (second and fourth columns) snapshots at 70 hPa of temperature (K), chlorine species (ppbv) and ozone (ppmv) for the Antarctic. First and second columns: selected example from the 1960 simulation. Third and fourth columns: selected example from the 2000 simulation. Note that for the chlorine species, the 1960 color bar ranges from 0 to 0.7 ppbv, while the 2000 color bar ranges from 0 to 2.8 ppbv.

in 1960. In the 1960 simulation, less nitrogen is bound in $ClONO_2$ and the ratio of NO2 to ClO is much larger. Formation of HNO_3 by $ClONO_2 + H_2O \rightarrow HNO_3 + ClOH$ (and other heterogeneous reactions) and its removal by particle sedimentation is less in the 1960 than in 2000 simulation. Concerning total nitrogen (NO_Y), its amount is more or less the same in the 1960 and 2000 simulations despite of the increase of its source gas N_2O by about 8% because of compensation effects of heterogeneous chemistry which lead even to a decrease of HNO_3 in 2000 by about 10%. Concerning water vapor, in general there is more of it in the 2000 simulation (see Figure 1). Figure 14 in addition shows that dehydration might have occurred in the 2000 example (note the water vapor minimum collocated with the lowest temperature in the eastern Arctic), possibly as a consequence of lower Arctic minimum temperature (possible feedback from ozone depletion, here of about 2 K) with respect to the 1960 simulation.

[44] Figure 15 (October and November snapshots for either the 1960 and the 2000 simulations) shows that in the 1960 simulation there is chlorine activation in October in the Antarctic high latitudes, but ozone amounts remain high. In early November in the 1960 example it is too warm to form PSCs. In turn, chlorine nitrate reforms (second column, third row), because (despite de-nitrification on particles at the low chlorine) enough NO_X can form from the photolysis of HNO_3. This situation is very similar to that occurring in the Northern Hemisphere for the 1960 conditions (e.g., unperturbed atmosphere). In contrast, in the 2000 simulation even in early November, ozone is almost completely depleted at high latitudes (as it was show already in part 1). Note also the lower temperature in the 2000 cases, in contrast to the 1960 cases (difference of more than 10 K), the manifestation of the radiative-chemical feedback. The cooling is due to less absorption of solar radiation given the ozone depletion. This cooling allows for some PSC over the Wedell Sea, a feature also observed by the POAM satellite in 2001 [*Bevilacqua and the POAM Team*, 2002].

[45] Figure 15 also show that in Antarctica, the substantial ozone depletion leads to a distinct change in the temporal evolution of chlorine partitioning from the 1960 to the 2000 simulation. In the 2000 simulation the chlorine reservoir that recovers first is HCl (third and fourth column second row). The mechanism has been discussed by *Douglass et al.* [1995]. The very low ozone in 2000 favors the production of HCl ($Cl + CH_4 \rightarrow HCl + CH_3$) by a high Cl/ClO ratio and suppresses the production of $ClONO_2$ ($ClO + NO_2 \rightarrow ClONO_2$) because of a reduced $NO_2/(NO + NO_2)$ ratio and increases the reaction $ClO + NO \rightarrow Cl + NO_2$, which further boosts HCl production. The result is an almost complete conversion of Cl_Y (total inorganic chlorine) to HCl at polar latitudes, surrounded by a $ClONO_2$ collar (see also part 1 and reference there to observations). In contrast, ozone and $ClONO_2$ remain high and HCl low in the 1960 simulation in the November snapshots. HNO_3 is comparable in the two simulations (see part 1 for a snapshot from the 2000 simulation of HNO_3). As for the Northern Hemisphere, in the 1960 simulation at middle latitudes HNO_3 is slightly higher than in the 2000 simulation, since less NO_Y is tied up in $ClONO_2$.

[46] Figure 16 shows the mean area covered by NAT-PSCs in both hemispheres, together with its variability for

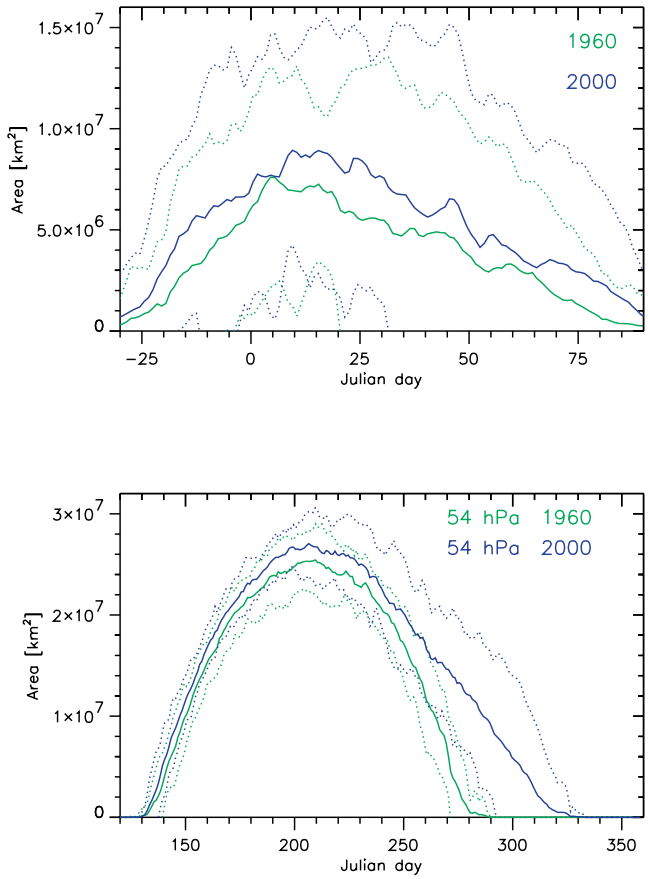

Figure 16. (top) Arctic and (bottom) Antarctic mean area covered with NAT-PSCs at the 54 hPa level from (green/light grey) the 1960 simulation and (blue/dark grey) the 2000 simulation. The dotted lines show the respective range covered by ±2 standard deviations. Note the different x-y axis scaling.

both the 1960 and 2000 simulations. It demonstrates that the feedback on the temperature by ozone depletion substantially enhances the mean area, the persistence, and the interannual variability of the PSCs in Antarctica in late spring. In November this change is highly significant (see also Figure 11). A similar change is found also for the PSCs in the Arctic, although it is partially overcome by the interannual variability due to internal dynamics, typical of the Northern Hemisphere. In middle to late March also in the Arctic the PSC change is significant, the average area more than doubles. This result is consistent with the mean temperature change in Figure 5. In the 2000 simulation there are 12 out of 20 years where polar stratospheric clouds (PSCs) are still present in late March while for the 1960 simulation PSCs in late March are found only in 6 out of 20 years. The 2000 scenario also contains more very cold polar winters and springs with dehydration than the 1960 scenario (as noted earlier).

7. Dynamical Activity and Interannual Variability

[47] A way to illustrate the dependence of the polar lower stratospheric temperature to the dynamical activity in the

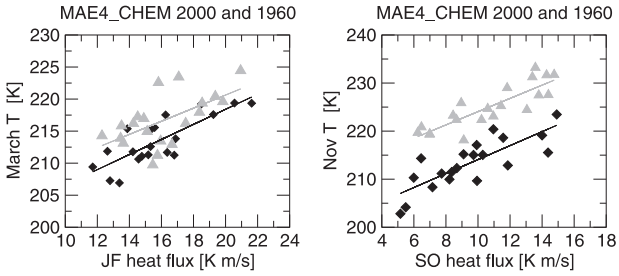

Figure 17. Scatterplot of (left) January–February meridional heat flux at 100 hPa (40°–80°N area weighted average) and March temperature at 50 hPa (60°–90°N area weighted average); and (right) September–October meridional heat flux at 100 hPa (40°–80°S area weighted average) and November temperature at 50 hPa (60°–90°S area weighted average). Each symbol is a mean from an individual year. Light triangles and line are for the 1960 simulation. Dark diamonds and line are for the 2000 simulation.

troposphere is to present scatterplots of temperature at 50 hPa and eddy heat flux at 100 hPa, averaged over convenient areas and time periods, following *Newman et al.* [2001]. Figure 17 shows such scatterplots for the northern and southern polar caps, respectively.

[48] The 1960 and 2000 January–February (JF) meridional eddy heat fluxes for the Northern Hemisphere (left) range from 11 to 22 K m/s for both simulations. These model results are comparable to the meridional heat fluxes computed from the NCEP reanalysis, *Newman et al.* [2001] and also part 1. Throughout the range of the heat fluxes, the March temperatures tend instead to be lower for the 2000 simulation, as shown by the downward displacement (not statistically significant) of the regression line, without substantial change in its slope. This result is indirect evidence that the radiative temperature is lower in the 2000 simulation, because the temperature range is lower for the same range of the heat fluxes. By extrapolation of the regression line to zero fluxes, it is estimated a radiative temperature of 195 ± 3 K for the 2000 simulation and of 200 ± 5 K for the 1960 simulation. The actual 2000–1960 change in March temperature, area weighted average poleward of 60°N is about −3 K at 50 hPa (i.e., slightly less than that in Figure 5, which shows the temperature change at 80°N). Within the uncertainties, the actual and estimated changes are comparable. These results are consistent with the average vertical EP-flux shown in Figure 7 and the interpretation introduced in section 5.1, that the dynamical forcing of the troposphere to the stratosphere does not play a dominant role in determining the 2000–1960 temperature change in March in the lower stratosphere.

[49] The range spanned by the 1960 and 2000 September–October (SO) meridional heat fluxes (5 to 15 K m/s) in the Southern Hemisphere is also very similar in the two simulations. Note that the heat fluxes are weaker than in the Northern Hemisphere, because of the weaker planetary wave activity emerging from the southern troposphere. In this case, the downward shift of the regression line is quite pronounced (significant at the 99% level), indicating a clear decrease in the estimated radiative temperature of 10 K. A difference of ∼10 K is also found for the actual 2000–1960 change in November temperature, area weighted average poleward of 60°N at 50 hPa, supporting the interpretation that the reported changes in the lower stratosphere are mainly due to the radiative response of the atmosphere to the chemical ozone depletion.

[50] Concerning changes in the 20-year average of the vertical EP flux in the southern polar cap, it is found that consistently with the local cooling and the local decrease in lower stratosphere downwelling, at 100 hPa the vertical EP flux is reduced from September to November, of about half a standard deviation. However, it is hardly changed at 300 hPa. The average meridional EP flux indicates a relatively large (up to one standard deviation) increase in the equatorward wave propagation in the 2000 simulation (with respect to the 1960), from September to December and at both 100 and 300 hPa. It would therefore be of interest to further analyze the simulation to establish if in this case the cooling due to ozone depletion is indeed inducing a change in the wave propagation characteristics of the troposphere.

[51] It is worth noting anyway that in Figure 17 the monthly mean heat fluxes appear to cluster toward low values in the 2000 simulation. This clustering appears in both hemispheres (slightly more in the Southern Hemisphere) and is consistent with the suggestion of a feedback of ozone depletion on the occurrence of months with weak fluxes. However, much longer simulations than those that can be performed nowadays with chemistry climate models would be necessary to demonstrate such a feedback in a statistical sense. This investigation is beyond the focus of this work and is left for further studies.

[52] The day-to-day and year-to-year variability of the northern and southern polar vortices is illustrated by the temporal evolution of the daily 30 hPa North Pole temperature, repeated for each year of the 1960 and 2000 simulations (Figure 18). Very little variability (day-to-day as well as year-to-year) is found in summer and early autumn at both poles and all simulations. Typically, when the temperature decreases in autumn as expected by the lack of solar heating, variations in the temperature start to occur, as large as 50 K in northern midwinter, both within one season (few days to two weeks) and interannually. These large variations in temperature are the so-called sudden stratospheric warming events [*Andrews et al.*, 1987]. No appreciable difference in the occurrence in sudden stratospheric warming events is visible from Figure 18 for the Northern Hemisphere.

[53] As it is well known, variability in the Southern Hemisphere is not as pronounced as that in the Northern Hemisphere. The individual years of both the 1960 and 2000 simulations are indeed characterized by midwinter temperatures that are very low and clustered around the average. Only in October and November the interannual variability becomes relatively substantial. It is noted an average shift in the temperature during spring. In addition, a couple of years are considerably above, and another couple of years considerably below the rest of the curves, a suggestion that there might be an overall increase in variability in the 2000 simulation, due to the chemical, radiative and dynamical coupling.

[54] Interannual variability of total ozone (for grid points corresponding to a station in the Arctic and one in the Antarctic) and its change between the 1960 to the 2000

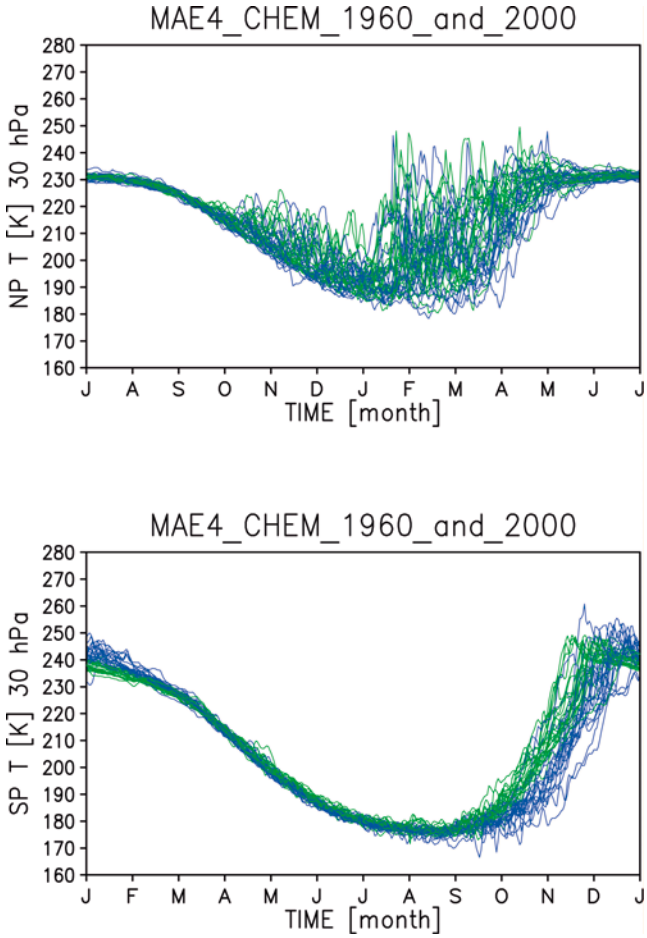

Figure 18. Daily temperature at 30 hPa at (top) North Pole and (bottom) South Pole. Green color (light grey) is for the 1960 simulation, and blue (dark grey) is for the 2000 simulation.

simulations is shown in Figure 19 and compared with ground based and satellite observations. Concerning the Arctic grid point, within the 2000 simulation and the observations of the late nineties there are some extreme cases with very low total ozone, an indication that the occurrence of ozone depletion has the potential to increase the interannual variability of the atmosphere. The change for the Antarctic grid point is dramatic, in both the seasonal

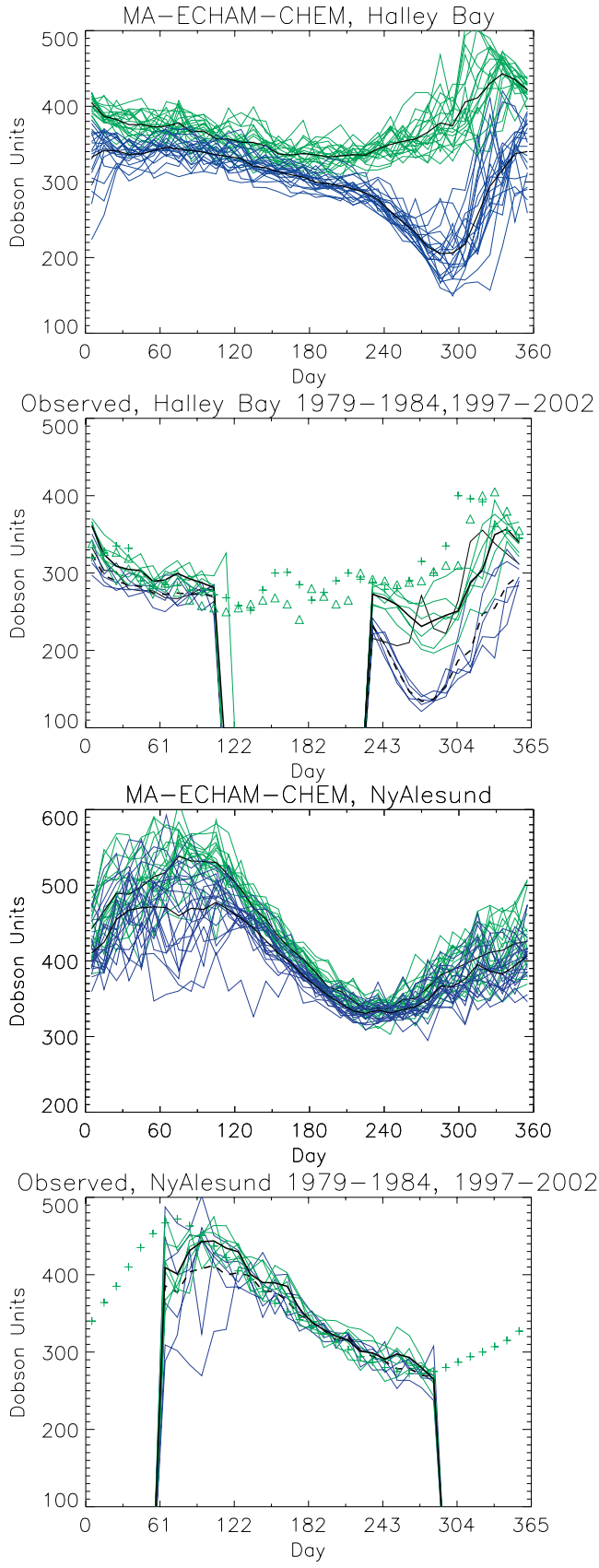

Figure 19. (opposite) Total ozone (DU) at the model grid points corresponding to (top) Halley Bay (76°S, 25°W) and to (bottom) Ny Alesund (79°N, 10°E) compared to observations. First and third panels: (green/light grey) from the 1960 simulation and (blue/dark grey) from the 2000 simulation. The curves are from 10-day averages of the individual years. Black curves are the 20-year averages. Second and fourth panels: The symbols are observations in 1957 and 1958 taken from *Dobson* [1968]. 10-day average TOMS-data from 1979 to 1984 are shown as green (light grey) curves, from 1997 to 2002 as blue (dark grey) curves (no data for polar night). Thick black curves are the respective averages. The 2002 data in Antarctica shown in thin black are excluded in the average.

cycle of the average amount of total ozone (another visualization of what is shown in Figure 2) and in the range of variability. Already by visual inspection, it is clear from Figure 19 that the range of total ozone values spanned around day 330 in the 2000 simulation is twice as large that spanned in the 1960 simulation. Except for the high total ozone bias discussed in part 1, the model captures the observed changes in seasonal cycle and variability.

8. Summary and Conclusions

[55] A middle atmosphere climate model with interactive chemistry has been employed for multiyear simulations with fixed boundary conditions for near-past and present conditions. Specifically, results from three 20-year equilibrium simulations have been presented: The 1960 simulation for near-past condition, characterized by low chlorine and greenhouse gases concentrations, and the 1990 and 2000 simulations with respectively chlorine and greenhouse gases concentration of the early and late 1990s. Climatological sea surface temperatures have been specified for each simulation. Most of the results reported here covered the 1960 and 2000 simulations.

[56] The main findings of this work are summarized as follows:

[57] 1. The atmosphere in the 2000 simulation is globally perturbed with respect to the atmosphere in the 1960 simulation, as shown by the 2000–1960 change in the annual, zonal mean ozone, temperature and water vapor. These average changes are consistent with the observed trends in ozone and temperature as well as previous modeling works (see references in section 3).

[58] 2. In the Arctic stratosphere, a significant cooling in March with respect to the 1960 simulation is found only for the 2000 simulation. The difference in the responses of the 1990 and 2000 simulations is mainly due to larger dynamical forcing in the 1990 simulation with respect to both the 2000 and 1960 simulations. Therefore if there is any influence from ozone depletion, this influence can be easily masked. Tropospheric wave activity in January and February is instead comparable in the 1960 and 2000 simulations, suggesting that ozone depletion and greenhouse gases increase contribute to the 2000–1960 March cooling in the lower stratosphere. In addition, the thermal and dynamical 2000–1960 changes in the Arctic are qualitatively similar to those found in the Antarctic, for which the length of the simulations are enough to give significance at the 99% level. These results therefore provide support to the interpretation that the extreme low Arctic temperatures observed in March in the last decade can arise from radiative and chemical processes. Note that ozone radiation feedback might be facilitated in the Arctic in March because the vortex is often off the pole and therefore in part sunlit. Although variations in the lower stratospheric temperatures by low-frequency modulation of upward propagating wave activity from the troposphere cannot be ruled out, it does not seem to be a necessary factor in our simulations. In March, the 2000–1960 decrease in downwelling in the region of cooling may further reduce the temperature by reduced dynamical heating, providing a positive feedback to ozone depletion [*Austin et al.*, 1992; *Shindell et al.*, 1998].

[59] 3. In the Antarctic, the ozone hole develops in both the 1990 and 2000 simulations. The cooling of the lower stratosphere and the associated changes in zonal winds are highly significant and substantially larger and longer lasting than in the Arctic. In November and December, significant changes in zonal wind range from the lower mesosphere to the ground, providing evidence for a substantial perturbation of the atmospheric flow. Interestingly, a strengthening of the tropospheric westerlies in December has been recently inferred for the Southern Hemisphere from NCEP/NCAR reanalysis [*Thompson and Solomon*, 2002]. In a future work, it would be of interest to investigate the relevance of these changes for the troposphere with this model.

[60] 4. A novel result that emerges from the comparison of the 1960 and 2000 simulations is an increase in downwelling in the mesosphere at the time of cooling in the lower stratosphere (in March in the Arctic; in October in the Antarctic). The mesospheric increase in downwelling can be explained as the response of the gravity waves to the stronger winds associated with the cooling in the lower stratosphere. The behavior of the gravity waves is explained by the fact that strong stratospheric westerlies (e.g., the 2000 simulation) imply enhanced filtering of eastward gravity waves and therefore a net gravity wave momentum flux at the stratopause that is more negative than in the case of weak westerlies (e.g., the 1960 simulation). Assuming an isotropic gravity wave spectrum emerging from the lower troposphere, this is a general and reasonable result not restricted to the particular gravity wave parameterization used, although its details and the strength of the response can depend on the parameterization employed. Planetary waves appear to contribute to the downward shift of the increased downwelling, with a delay of about a month. It is plausible that the increased heating associated with the increased downwelling and its downward shift may limit the cooling and the strengthening of the lower stratospheric polar vortex from above, therefore facilitating ozone recovery and providing a negative dynamical feedback. Although significant changes in the zonal wind are found only for the Antarctic, the same behavior is found also in the Arctic. The difference in the change in downwelling in the two hemispheres stems primarily from the different average states, a consequence of the more active planetary waves in the Northern Hemisphere.

[61] 5. Because of the cooling in the lower stratosphere in the 2000 simulation, in both hemispheres the area covered with PSCs increases significantly in spring, contributing to the chemical-radiative-dynamical feedbacks. Chlorine partitioning in polar springs changes strongly from the 1960 to the 2000, while for the amount of total reactive nitrogen the increase from the N_2O increase is approximately compensated by enhanced de-nitrification.

[62] The reported changes in the mesosphere motivate the development of models with tops in the upper atmosphere, for use in climate change assessments. Currently, this type of model still has a crude representation of mesospheric processes. In the MAECHAM4/CHEM model, the upper mesosphere is essentially a buffer zone. Nevertheless, the effects of gravity wave breaking have been here taken into account in a comprehensive way, by using a parameterization that considers a spectrum of gravity waves. However, the forcing of the gravity waves was not changed between

the simulations, while it might if the meteorological variability of the troposphere does change. In a natural extension of this work, it would therefore be of interest to specify the forcing of the gravity waves from the simulated meteorological disturbances.

[63] **Acknowledgments.** We are grateful to L. Bengtson and P. Crutzen for their role in initiating and encouraging this work and G. P. Brasseur, K. Labitzke, E. Roeckner, and H. Schmidt for reading the manuscript. We would like to thank the anonymous reviewers for their constructive comments, which have helped us to improve the manuscript. Part of this work was supported by the German Research Ministry for Education and Research (BMBF) in the framework of the AFO2000 Program, KODYACS and MEDEC projects.

References

Andrews, D. G., J. R. Holton, and C. B. Leovy, *Middle Atmospheric Dynamics*, 489 pp., Academic, San Diego, Calif., 1987.

Austin, J., A three-dimensional coupled chemistry-climate model simulation of past stratospheric trends, *J. Atmos. Sci.*, *59*, 218–232, 2002.

Austin, J., N. Butchart, and K. P. Shine, Possibility of an Arctic ozone hole in a doubled-CO_2 climate, *Nature*, *360*, 221–225, 1992.

Austin, J., J. Knight, and N. Butchart, Three dimensional chemical model simulations of the ozone layer: 1979–2015, *Q. J. R. Meteorol. Soc.*, *126*, 1533–1556, 2000.

Austin, J., N. Butchart, and J. Knight, Three dimensional chemical model simulations of the ozone layer: 2015–2055, *Q. J. R. Meteorol. Soc.*, *127*, 956–974, 2001.

Austin, J., et al., Uncertainties and assessments of chemistry-climate models of the stratosphere, *Atmos. Chem. Phys.*, *3*, 1–27, 2003.

Bevilacqua, R., and the POAM Team, The Polar Ozone and Aerosol Measurement (POAM II and III) experiments: An overview of observations of polar ozone and related constituents and phenomenology, paper presented at EGS-Assembly, Eur. Geophys. Soc., Nice, France, 2002.

Brasseur, G. P., and S. Solomon, *Aeronomy of the Middle Atmosphere*, 2nd ed., D. Reidel, Norwell, Mass., 1986.

Brühl, C., K. Carslaw, T. Peter, J.-U. Grooß, J. M. Russell III, and R. Müller, Chlorine activation and ozone depletion in the Arctic vortex of the four recent winters using a trajectoriy box model and HALOE satellite observations, in *Atmospheric Ozone: Proceedings of the Quadriennial Ozone Symposium 1996*, vol. 2, edited by R. D. Bojkov and G. Visconti, pp. 675–678, Int. Ozone Comm., L'Aquila, Italy, 1998.

Butchart, N., and A. A. Scaife, Removal of chlorofluorocarbons by increased mass exchange between the stratosphere and troposphere in a changing climate, *Nature*, *410*, 799–802, 2001.

Dobson, G. M. B., Forty years' research on atmospheric ozone at Oxford: A history, *Appl. Opt.*, *7*, 387–405, 1968.

Douglass, A. R., M. R. Schoeberl, R. S. Stolarski, J. W. Waters, J. M. Russell III, A. E. Roche, and S. T. Massie, Interhemispheric differences in springtime production of HCl and $ClONO_2$ in the polar vortices, *J. Geophys. Res.*, *100*, 13,967–13,978, 1995.

Farman, J. C., B. G. Gardiner, and J. D. Shanklin, Large losses of total ozone in Antarctica reveal seasonal ClOx/NOx interaction, *Nature*, *315*, 207–210, 1985.

Fels, S. B., J. D. Mahlman, M. D. Schwarzkopf, and R. W. Sinclair, Stratospheric sensitivity to perturbations in ozone and carbon dioxide: Radiative and dynamical response, *J. Atmos. Sci.*, *37*, 2265–2297, 1980.

Fioletov, V. E., G. E. Bodeker, A. J. Miller, R. D. McPeters, and R. Stolarski, Global and zonal total ozone variations estimated from ground-based and satellite measurements: 1964–2000, *J. Geophys. Res.*, *107*(D22), 4647, doi:10.1029/2001JD001350, 2002.

Fleming, E. L., S. Chandra, J. J. Barnett, and M. Corney, Zonal mean temperature, pressure, zonal wind and geopotential height as function of latitude, *Adv. Space Res.*, *10*(12), 1211–1259, 1990.

Gillett, N. P., M. R. Allen, and K. D. Williams, The role of stratospheric resolution in simulating the Arctic Oscillation response to greenhouse gases, *Geophys. Res. Lett.*, *29*(10), 1500, doi:10.1029/2001GL014444, 2002.

Haynes, P. H., C. J. Marks, M. E. McIntyre, T. G. Shepherd, and K. P. Shine, On the "downward control" of extratropical diabatic circulations by eddy-induced mean zonal forces, *J. Atmos. Sci.*, *48*, 651–678, 1991.

Hines, C. O., Doppler spread parameterization of gravity wave momentum deposition in the middle atmosphere. Part 1: Basic formulation, *J. Atmos. Sol. Terr. Phys.*, *59*, 371–386, 1997a.

Hines, C. O., Doppler spread parameterization of gravity wave momentum deposition in the middle atmosphere. Part 2: Broad and quasi monochromatic spectra and implementation, *J. Atmos. Sol. Terr. Phys.*, *59*, 387–400, 1997b.

Kiehl, J. T., B. A. Boville, and B. P. Briegleb, Response of a general circulation model to a prescribed Antarctic ozone hole, *Nature*, *332*, 501–504, 1988.

Labitzke, K., and H. van Loon, A note on trends in the stratosphere: 1958–1992, in *Solar-Terrestrial Energy Program: The Initial Results From STEP Facilities and Theory Campaigns, Proceedings of the 1992 STEP Symposium/5th COSPAR Colloquium Held in Laurel, Maryland, U.S.A., 24–28 August 1992*, *COSPAR Colloq. Ser.*, vol. 5, pp. 537–546, Pergamon, New York, 1994.

Langematz, U., An estimate of the impact of observed ozone losses on stratospheric temperature, *Geophys. Res. Lett.*, *27*, 2077–2080, 2000.

Langematz, U., M. Kunze, K. Krüger, K. Labitzke, and G. L. Roff, Thermal and dynamical changes of the stratosphere since 1979 and their link to ozone and CO_2 changes, *J. Geophys. Res.*, *108*(D1), 4027, doi:10.1029/2002JD002069, 2003.

Mahlman, J. D., J. P. Pinto, and L. J. Umscheid, Transport, radiative, and dynamical effects of the Antarctic ozone hole: A GFDL SKYHI model experiment, *J. Amos. Sci.*, *51*, 489–508, 1994.

Manzini, E., and N. A. McFarlane, The effect of varying the source spectrum of a gravity wave parameterization in a middle atmosphere general circulation model, *J. Geophys. Res.*, *103*, 31,523–31,539, 1998.

Manzini, E., N. A. McFarlane, and C. McLandress, Impact of the Doppler spread parameterization on the simulation of the middle atmosphere circulation using the MA/ECHAM4 general circulation model, *J. Geophys. Res.*, *102*, 25,751–25,762, 1997.

Molina, L. T., and M. J. Molina, Production of Cl_2O_2 from the self-reaction of the ClO radical, *J. Phys. Chem.*, *91*, 433–436, 1987.

Naujokat, B., K. Krüger, K. Matthes, J. Hoffmann, M. Kunze, and K. Labitzke, The early major warming in December 2001—exceptional?, *Geophys. Res. Lett.*, *29*(21), 2023, doi:10.1029/2002GL015316, 2002.

Newman, P. A., E. R. Nash, and J. E. Rosenfield, What controls the temperature of the Arctic stratosphere during the spring?, *J. Geophys. Res.*, *106*, 19,999–20,010, 2001.

Pawson, S., et al., The GCM-Reality Intercomparison Project for SPARC (GRIPS): Scientific issues and initial results, *Bull. Am. Meteorol. Soc.*, *81*, 781–796, 2000.

Ramaswamy, V., et al., Stratospheric temperature trends: Observations and model simulations, *Rev. Geophys.*, *39*, 71–122, 2001.

Randel, W. J., and F. Wu, Cooling of the Arctic and Antarctic polar stratospheres due to ozone depletion, *J. Clim.*, *12*, 1467–1479, 1999a.

Randel, W. J., and F. Wu, A stratospheric ozone data set for global modelling studies, *Geophys. Res. Lett.*, *26*, 3089–3092, 1999b.

Rasch, P. J., and M. Lawrence, Recent development in transport methods at NCAR, *MPI-Rep. 265*, pp. 65–75, Max-Planck-Inst. für Meteorol., Hamburg, Germany, 1998.

Rosenlof, K. H., Transport changes inferred from HALOE water and methane measurements, *J. Meteorol. Soc. Jpn.*, *80*, 831–848, 2002.

Rosenlof, K. H., et al., Stratospheric water vapor increases over the past half-century, *Geophys. Res. Lett.*, *28*, 1195–1198, 2001.

Rozanov, E. V., M. E. Schlesinger, and V. A. Zubov, The University of Illinois, Urbana-Champaign three-dimensional stratosphere-troposphere general circulation model with interactive ozone photochemistry: Fifteen-year control run climatology, *J. Geophys. Res.*, *106*, 27,233–27,254, 2001.

Schnadt, C., M. Dameris, M. Ponater, R. Hein, V. Grewe, and B. Steil, Interaction of atmospheric chemistry and climate and its impact on stratospheric ozone, *Clim. Dyn.*, *18*, 501–517, 2001.

Shindell, D. T., D. Rind, and P. Lonergan, Increased polar stratospheric ozone losses and delayed eventual recovery owing to increasing greenhouse-gas concentrations, *Nature*, *392*, 589–592, 1998.

Shine, K. P., On the modelled thermal response of the Antarctic stratosphere to a depletion of ozone, *Geophys. Res. Lett.*, *13*, 1331–1334, 1986.

Shine, K. P., et al., A comparison of model-simulated trends in stratospheric temperatures, *Q. J. R. Meteorol. Soc.*, *129*, 1565–1588, 2003.

Solomon, S., Stratospheric ozone depletion: A review of concepts and history, *Rev. Geophys.*, *37*, 275–316, 1999.

Steil, B., M. Dameris, C. Brühl, P. J. Crutzen, V. Grewe, M. Ponater, and R. Sausen, Development of a chemical module for GCMs: First results of a mutli-annual integration, *Ann. Geophys.*, *16*, 205–228, 1998.

Steil, B., C. Brühl, E. Manzini, P. J. Crutzen, J. Lelieveld, P. J. Rasch, E. Roeckner, and K. Krüger, A new interactive chemistry-climate

model: 1. Present-day climatology and interannual variability of the middle atmosphere using the model and 9 years of HALOE/UARS data, *J. Geophys. Res.*, *108*(D9), 4290, doi:10.1029/2002JD002971, 2003.

Thompson, D. W., and S. Solomon, Interpretation of recent Southern Hemisphere climate change, *Science*, *296*, 895–899, 2002.

Waugh, D. W., W. J. Randel, S. Pawson, P. A. Newman, and E. R. Nash, Persistence of the lower stratospheric polar vortices, *J. Geophys. Res.*, *104*, 27,191–27,201, 1999.

World Climate Research Program-Stratospheric Processes and their Role in Climate (WCRP-SPARC), Assessment of trends in the vertical distribution of ozone, *Rep. 1*, Geneva, 1998.

World Meteorological Organization (WMO), Scientific assessment of ozone depletion: 1994, *Rep. 37*, Geneva, 1995.

World Meteorological Organization (WMO), Scientific assessment of ozone depletion: 1998, *Rep. 44*, Geneva, 1999.

C. Brühl and B. Steil, Max-Planck-Institut für Chemie, P. O. Box 3060, D-55020 Mainz, Germany. (chb@mpch-mainz.mpg.de; steil@mpch-mainz.mpg.de)

M. A. Giorgetta, Max-Planck-Institut für Meteorologie, Bundesstraße 55, D-20146 Hamburg, Germany. (giorgetta@dkrz.de)

K. Krüger, Institut für Meteorologie, Freie Universität Berlin, Carl-Heinrich-Becker-Weg 6-10, D-12165 Berlin, Germany. (krueger@strat01.met.fu-berlin.de)

E. Manzini, National Institute for Geophysics and Volcanology, Via Creti 12, I-40128 Bologna, Italy. (manzini@bo.ingv.it)